AN APPROXIMATE THEORY FOR POTENTIAL FLOW THROUGH CASCADES OF AIRFOILS

Thesis by

George E. Hlavka

In Partial Fulfillment of the Requirements

For the Degree of

Doctor of Philosophy

California Institute of Technology

Pasadena, California

1954

ACKNOWLEDGMENTS

The author wishes to express his sincere appreciation to Dr. W. D. Rannie, under whose guidance this work was done. His intimate knowledge of the field of turbomachinery was of invaluable assistance in the formulation and solution of the problem treated herein.

Much was also gained from discussions with Dr. H. S. Tsien and Dr. F. E. Marble of the Guggenheim Jet Propulsion Center. Dr. A. Erdélyi and Dr. H. F. Bohnenblust gave helpful advice regarding the mathematical analysis.

Financial assistance was afforded in the form of a Daniel and Florence Guggenheim Foundation Fellowship in Jet Propulsion.

A final word of appreciation is due to Miss Janet Chandler for assistance with the computations, and to Miss Ruth Winkel for typing the manuscript.

ABSTRACT

A new analytic theory is presented for predicting certain characteristics of the plane potential flow through a cascade. The analysis is based on the assumption that the airfoils of the cascade deviate only slightly from straight lines.

The theory provides a means for obtaining higher order approximations than have been found heretofore. As a result it has been possible to evaluate the accuracy of existing first-order approximations.

In addition the first-order theory has been extended by the addition of a means for obtaining the variation of flow velocity and pressure at the airfoils, and the removal of certain restrictions on angle of attack.

TABLE OF CONTENTS

REVIEW AND SUMMARY

This investigation is concerned with plane potential flow through a cascade of airfoils. A new analytic theory is presented, by means of which one can predict certain characteristics of the flow and obtain insight into the effect of some of the many variables involved.

A sizable literature exists on this subject, though very little of it is actually useful. The work of Weinig, Pistolesi, Klingemann, and Garrick deserves mention, however.

The first comprehensive treatise on plane potential flow through cascades is "Die Strömung um die Schaufeln von Turbomaschinen", published by Weinig[1] in 1935. This work deserves considerable praise for the wealth of information it contains and the care with which it is presented. The book has become a standard reference in its field and subsequent work has often verified its conclusions. In addition to discussions of a large number of special cases, a method is outlined for treating cascades with arbitrary airfoils. Actually the special cases are of value principally for insight into the problem, and little use has been made of the method for arbitrary cascades. For the designer of an axial flow compressor, the useful items in Weinig's book are some relations for flow with smooth entry at the leading edges of the airfoils of one type of cascade. The camber and airfoil orientation are given for the smooth entry condition for cascades with zero-thickness circular arc airfoils. Though the airfoils in an actual cascade must have some thickness, the Weinig relations are nevertheless used if the camber line (or mean line) has the form of a circular arc.

In 1937 Pistolesi[2] published an approximate solution of the

cascade problem in the form of an involved extension of the Birnbaum-Glauert thin airfoil theory for a single airfoil with small angle of attack[3]. His equations have had virtually no practical use because of their complexity. Furthermore the assumptions of Birnbaum and Glauert, which Pistolesi used, introduce greater errors in the cascade theory than in the original application to single airfoils as is shown for the first time in the present paper. For example his results for the simple flat plate cascade do not agree with the known exact solution. Thus this frequently-quoted work represents no improvement over the results of Weinig.

Another analytic approximate solution of the cascade problem was published by Klingemann[4] in 1940. This ingenious theory combined the use of conformal transformation, which was the principal tool of Weinig, with the use of the Birnbaum model for the flow field, used in the Pistolesi theory. Since the exact flat plate cascade solution was used as a starting point, the results are more accurate than those of Pistolesi. Klingemann obtained a simple equation for the lift coefficient for a cascade of zero-thickness circular arc airfoils with small angle of attack. Actually the same equation can be obtained from Weinig's results for the same type of cascade; hence Klingemann's equation was essentially a verification of the work of Weinig. Klingemann also obtained an expression for the lift coefficient for the case of zero-thickness S-shaped airfoils, but this is much less tractable, being in the form of a series which is impractical to compute for low airfoil spacing. The treatment of S-shaped airfoils did, however, represent an advance beyond the work of Weinig.

The work of Garrick[5] published in 1944 is exemplary of a large number of solutions of the cascade problem which are essentially

numerical methods similar to the early method of Weinig. Applicable to any cascade geometry, the Garrick method enables the complete solution to be found. Several successive conformal transformations are involved, one of which is performed by the iterative numerical procedure of the single airfoil method of Theodorsen[6]. However the entire solution is very lengthy and laborious, particularly if reasonable accuracy is required. Furthermore each new cascade geometry must be treated individually.

In a sense the complete solution of the flow through an arbitrary cascade has therefore been obtained: the methods of Garrick and other recent investigators - or the original method developed by Weinig - can be used with any cascade geometry. The reasons for sustained interest in the problem are the shortcomings of these methods with regard to flexibility, simplicity, and accuracy. The relations of Weinig for smooth entry, and the results of Klingemann are more simple to use but are limited in range of application. The restriction to circular arc and S-shaped camber lines and combinations of these is not serious in view of present day practice, but the absence of any information about the influence of airfoil thickness is more important, since the flow velocity and static pressure at the airfoil are decidedly dependent upon thickness. Furthermore there is no information as to accuracy of the existing approximate theories.

This investigation was prompted by the need for a theory which would be less restrictive than the existing analytical theories, yet without the disadvantages of numerical methods. The resulting analysis differs from previous work in several important respects:

(1) The theory is based upon certain approximations and therefore differs from numerical methods such as that of Garrick. Even if the iterative numerical process of the Garrick method is simplified by using only the first approximation, there is still little resemblence to the present theory; the effects of thickness and camber line shape are treated separately in the latter, and only one conformal transformation is used.

(2) The present theory can be used to obtain second and higher order approximations, which were not obtained in the approximate theories of Pistolesi and Klingemann.

(3) The theory also differs from those of Pistolesi and Klingemann in that the Birnbaum model for the flow field is not used, and that no restriction is assumed on angle of attack.

The approximations of the present theory amount essentially to the assumption that the cascade airfoils differ little from straight lines. The flat plate cascade, for which the exact solution is known, is used as the zeroth approximation to the arbitrary cascade. Though applied in an entirely different manner, this is also the assumption used by Klingemann. In the present theory this assumption is used to obtain first-order terms in a transformation equation relating the cascade plane and a circle plane. Then these terms are used to obtain second-order terms, and so on.

The results of the present theory are equations for overall flow characteristics (such as lift coefficient and downstream flow direction) and the variation of velocity and pressure at the cascade airfoils. Two types of airfoil camber line are considered: circular arc (or symmetric parabola), and S-shaped. Combinations of these plus an arbitrary thick-

ness distribution are sufficiently general for the theory to be described as applicable to arbitrary cascades within the limits of the approximations involved.

An original objective of doing extensive work on the higher order approximations was curtailed when the complexity of the expressions involved was recognized. Certain untabulated functions of the complex variable (or equivalent complex integrals) were encountered. This was recognized as a limitation to the usefulness of the higher order results.

However some success was obtained when certain additional approximations were applied to what were considered to be the most important higher order terms, namely, second-order terms due to airfoil camber. The resulting expressions were used in an error analysis and led to a simple expression for maximum error of the first-order approximations to certain flow characteristics. It was also found from the second-order terms that the first-order equation for flow characteristics giving downstream flow angle were numerically more accurate than the first-order equations for other flow characteristics such as lift coefficient.

Thus the majority of equations derived in this thesis are first-order approximations and frequently duplicate the earlier results of Weinig and Klingemann. However certain improvements of the existing first-order theories have been made:

(1) The restrictions on angle of attack have been removed.

(2) The results for S-shaped camber lines are in more tractable form than those of Klingemann.

(3) The inaccuracy of Pistolesi's equations have been pointed out and analysed.

(4) The effect of thickness on velocity distribution has been established.

(5) The accuracy of first-order equations has been determined.

The last two are, of course, the most important.

One final interesting point deserves mention here. A comparison with a well-known empirical formula indicated that the present first-order results for zero-thickness airfoil cascades are in fair agreement with results for actual test cascades having normal airfoil thickness. There are also indications that the new analytically derived formula may be an improvement over existing empirical rules.

I. INTRODUCTION

The design of a turbomachine and the prediction of its performance require knowledge of the internal fluid flow. Current design trends indicate that turbomachines of the future will be smaller than present machines. This means higher energy transfer and greater turning of the flow, and provides an incentive for more research on the flow problem.

For axial flow machines it is frequently assumed for simplicity that the stream surfaces are cylindrical. Since a cascade is an infinite row of airfoils, circumferential sections of the flow through a row of rotor or stator blades can then be considered as plane cascade flow. For design purposes cascades are considered at several radial stations; the resulting airfoil sections are used to construct the blades. With the blade geometry fixed the off-design performance can also be predicted (to a more limited extent) from cascade performance.

It has been found in practice that two-dimensional cascade flow represents a good approximation to the actual flow at all radii except at the blade extremities, where boundary layer and secondary flow phenomena are important. The latter influences are not yet fully understood, hence most compressors are still designed ignoring these three-dimensional effects. Because the theory of the two-dimensional cascade is far from complete, many designers use only experimental data from cascade tests. The object of the present investigation is to improve the usefulness of the cascade theory, both for design purposes and to aid interpretation of cascade tests.

A cascade is a row of equally spaced airfoils. A typical compressor cascade is shown in Figure 1. Also shown are some streamlines of the flow and the chord and camber lines.

Differences exist as to the precise meaning of the terms chord, camber line and airfoil thickness. This will be illustrated by a description of several ways an airfoil shape may be constructed. The chord line is straight and of length equal to the chord; its ends are called the leading edge and the trailing edge (Figure 1). The camber line is (in general) curved and also connects the leading and trailing edges. The profile of the airfoil may be obtained by adding a thickness distribution to the camber line in either of two ways: normal to the chord line[7], or normal to the camber line[8],[9]. The thickness distribution is zero at the leading and trailing edges and may be a function of position on the chord line or on the camber line. Thus if the airfoil profile is given, and used to find the chord and the camber line, the results will depend on the method of construction assumed. Fortunately the differences are usually small and in any approximate theory, such as that to be described here, can be neglected.

The most useful characteristics of flow in a cascade are: (1) those which describe the overall effect of the cascade on an approaching uniform flow, and (2) those which describe in more detail the flow at the surface of each airfoil. Examples of the first type are circulation, lift coefficient, deviation angle, downstream flow direction, and flow turning angle; all of these are a measure of the same effect and are therefore related. The second type of flow characteristic, generally more difficult to determine, is exemplified by velocity and pressure distribution on the airfoils.

Cascade problems are usually classified according to two types: the direct problem and the inverse problem. The direct problem

consists of determining the flow characteristics of a given cascade; the inverse problem consists of determining the cascade geometry from certain given flow characteristics. This thesis is primarily concerned with the former problem, although the results can also be used for an important example of the latter.

A considerable amount of work has been done on direct cascade problems in the past. A detailed account of each method of solution would be out of place here. However a brief indication of the basic principles will be given, since the points of departure of the present work can then be seen.

A. The Single Airfoil Problem

The cascade problem is directly related to the single airfoil problem of aeronautics. In fact the latter can be regarded as a limiting case of the former (that of infinite airfoil spacing). Also some of the methods of solving the cascade problem are extensions of single airfoil methods. Thus a discussion of methods of solution of the single airfoil problem is appropriate.

Complete exact solutions of the flow problem have been obtained in certain special cases with the use of conformal transformation. Briefly the method consists of considering the physical problem in the plane of one complex variable (where the solution is readily obtained), followed by interpretation of the results in the original plane[10], [11], [12]. The two planes are related by a transformation equation, which must be determined for each problem. The simplest case is the flat plate airfoil, which is transformed into a circle. The transformation for this case is an important one called the Joukowski transformation. If w

is the physical plane (the plane of the airfoil) and ζ is the circle plane, the equation relating the w and ζ planes is

$$w(\zeta) = \frac{1}{4}\left(\zeta + \frac{1}{\zeta}\right) \tag{1}$$

which connects a unit circle in the ζ plane and a flat plate of unit chord in the w plane. Equation (1) can also be used for elliptic airfoils and a family called Joukowski airfoils[13], [14] if other circles are chosen in the ζ plane. Relatively simple exact equations have been obtained in these cases for such flow characteristics as lift coefficient and velocity distribution on the airfoils.

For the single airfoil of arbitrary shape no complete analytical solution of the flow problem exists, though numerous numerical methods are available. One of the earliest attempts to obtain analytical results by an approximate method is that of Birnbaum[15], for airfoils of zero thickness. The method does not involve conformal transformation; instead a model is established to represent the airfoil in the flow field. The model consists of a vortex distribution on the airfoil chord line, and the complete flow field is approximated by adding the contribution due to this vortex distribution to a uniform flow. A method of determining the vortex distribution for a given camber line was subsequently given by Glauert[3] who used the approximate relation:

$$\text{slope of the camber line} = \alpha + \frac{V_{\text{VORTEX}}}{V_\infty} \tag{2}$$

where α is the angle of attack, V_{vortex} is the velocity at and normal to the chord line due to the vortex distribution, and V_∞ is the velocity far from the airfoil.

Birnbaum made no attempt to consider airfoil thickness. Actually if the effect of thickness is accounted for by adding a source-

sink distribution on the chord line, it is found that his first approximation to the overall flow characteristics is unchanged, due to the assumption of small angle of attack. Hence the Birnbaum theory is frequently regarded as a theory of airfoils of small thickness, a "thin airfoil" theory. However it is actually for airfoils of zero thickness, and gives infinite velocity at the leading edge[16], [17], an impossibility for an airfoil with a rounded nose.

Essentially the Birnbaum theory is a first order approximation to the exact solution of the single airfoil problem under the assumptions that airfoil thickness is zero, and that camber and angle of attack are small.

Another solution for the single airfoil of zero thickness is due to Rannie. Discussion of this method will be found in the last section of this Introduction since it has direct bearing on the method to be described in this paper.

Recently Lighthill[17] has published a refinement of the Birnbaum theory in which the difficulties with velocity at the leading edge have been overcome by properly accounting for thickness. Furthermore his technique can be used for second and higher order approximations. Limitations of small thickness, camber, and angle of attack remain, however.

In contrast to the Birnbaum theory in which no conformal transformations occur, there are other methods in which it is essential. One of these, due to Munk[18], leads to the same final relationships as the Birnbaum-Glauert theory. The latter theory is stressed here because the extensions to cascades have been based on the Birnbaum

model of the flow. Another well known method is due to Theodorsen[6], [11] and has been used with considerable success; it will now be described briefly.

The Joukowski transformation, Equation (1), can be used to transform a flat plate, an ellipse, or a Joukowski airfoil into a circle, about which the corresponding flow is easily established. If properly applied to an arbitrary airfoil, the resulting figure is nearly circular. In the Theodorsen method the nearly circular figure (in the ζ plane) is transformed into a circle (in the z plane) by a second transformation, given by

$$\zeta(z) = \sum_{n=0}^{\infty} \frac{A_n}{z^n} + z \qquad (3)$$

where the complex coefficients A_n must be determined, and are usually found by iterative numerical methods. The treatment of the flow problem after the circle has been obtained resembles that used for the simpler airfoils.

The Theodorsen theory is usually considered an exact numerical method for arbitrary airfoils. It is possible to simplify it somewhat by certain approximations. Goldstein[7], [19] has derived several formulas for velocity on an arbitrary airfoil, by linearizing the Theodorsen theory. His approximations lead to equations resembling those obtained later by Lighthill. The results are more simple than the exact results of Theodorsen, and do not have the leading edge difficulties of early thin airfoil theory. However the limitations of small thickness and small camber are present. The Goldstein method has not generally replaced the method of Theodorsen, possibly because the most accurate Goldstein equation is fairly complicated, and that computing machines have been

adapted to handle the numerical part of the Theodorsen method.

B. The Cascade Problem

The cascade problem is made more complicated than the single airfoil problem by the additional parameters airfoil spacing and stagger. However certain exact solutions are available, although as in the case of single airfoils they are generally of little interest except as a basis for an extension. The most familiar exact solution is that of the flat plate cascade[1], [5], [14] which uses the transformation equation

$$w(z) = \frac{\sigma}{\pi}\left[e^{i\beta}\tanh^{-1}\left(\frac{b_0}{z}\right) + e^{-i\beta}\tanh^{-1}(b_0 z)\right]. \tag{4}$$

This equation relates a unit circle in the z plane and a flat plate cascade of chord unity, spacing σ (solidity $\frac{1}{\sigma}$), and stagger angle β in the w plane (see Figure 2). Choice of β and the real parameter b_0 determine σ through the equation

$$\frac{\pi}{2\sigma} = \cos\beta \tanh^{-1}\left(\frac{2b_0\cos\beta}{Q}\right) + \sin\beta \tan^{-1}\left(\frac{2b_0\sin\beta}{Q}\right) \tag{5}$$

where

$$Q = +\sqrt{1 + b_0^4 + 2b_0^2\cos 2\beta}\,. \tag{6}$$

It is obvious that this transformation is considerably more complex than the Joukowski transformation, Equation (1).

The flat plate transformation equation given above has been used by Weinig[1] to derive Joukowski-like cascade airfoils, in an exact theory paralleling the Joukowski airfoil theory. The analysis is quite involved and the cascades have little practical significance,

though the results afford considerable insight into cascade flow.

A more important contribution by Weinig is his work on cascades with zero-thickness circular arc airfoils. Weinig determined the conditions under which the flow enters the cascade smoothly without infinite velocity at the leading edges. His results were used extensively in Germany for designing early axial flow compressors.

Another exact solution to be briefly mentioned here is the zero-spacing, zero-thickness cascade, which will be hereinafter referred to as the infinite solidity cascade. Here continuity considerations alone enable the solution to be obtained readily for any stagger or zero-thickness airfoil shape. Again the results are trivial, but they will be used here as an important limiting case for checking purposes.

For cascades with arbitrary airfoil shapes, various extensions of single airfoil theory have been devised. Analytical thin airfoil theories have been devised by several authors, and in each case a model similar to that of Birnbaum has been employed. Pistolesi[2] derived integral equations similar to those of Glauert for determining chordwise vortex distributions for a given camber line. He also considered the effect of small thickness. His equations are considerably more complex than those for single airfoils largely because of the introduction of spacing and stagger. Scholz[20] interpreted the results of Pistolesi, but added nothing new to the theory. Lieblein[21] extended the Pistolesi theory to include airfoils of small thickness with finite trailing edge angle. Hudimoto[22] conformally transformed the chord lines into a circle and considered the vortices to be located on the circle. Klingemann[4] also used the circle plane but considered a potential flow which crosses the circle.

All of the foregoing thin airfoil theories have limitations of small (or zero) thickness, small camber, and small angle of attack. For cascades these limitations are more serious than for the single airfoil:

(1) Though airfoil thickness has no effect on the first order approximation for lift coefficient of the single airfoil at small angle of attack, this is not true in general for the cascade, as shown by Pistolesi[2].

(2) The maximum camber encountered in a compressor cascade may be twice as large as for a single airfoil, while the ratio may be as high as four for a turbine cascade.

(3) Even for small angles of attack greater error is introduced by approximations similar to Equation (2), because in the cascade there is an additional component of velocity parallel to the chord due to the vortex distributions on the chord lines of neighboring airfoils.

In short the assumption that the airfoil deviates but little from a flat plate is much less adequate for the cascade, and the errors introduced by assuming singularities on the chord line (which may actually lie partly outside the airfoil as in Figure 1) can be considerably greater than for the single airfoil. These errors have never been systematically studied.

The innovation of Theodorsen, that of transforming the arbitrary airfoil into a near-circle by a flat plate transformation, followed by a transformation into a circle, has been applied to cascades by a number

of authors. One of the best known methods is that of Garrick[5], which will now be described.

In the Garrick method, Equation (4) is used to transform the airfoils into a single nearly circular curve. Then Equation (3) and the Theodorsen method are used to obtain a circle. In the first transformation the points at infinity in the physical plane are taken into the singular points $z = \pm 1/b_o$. In the second transformation the singular points are transformed into, in general, two unsymmetrically placed singular points. A third and final transformation (which is not necessary for the single airfoil) restores the symmetry of the singular points while retaining the circular form for what were the original airfoils. The flow problem is easily solved in the final circle plane and the numerical transformation relations are used to give the flow characteristics in the original physical plane. The labor involved can be reduced by the use of various numerical techniques[23], [24] or automatic computing machines.

Similar methods involving several successive conformal transformations to a circle have been devised by Howell[25], Traupel[26], Weinig[1], Kamimoto[22], Abe[27], Merchant[28], Lighthill[29], Hirose[30], Moriya[31], and others. These methods are all extensions of the Theodorsen numerical method to the cascade problem, and the apparently undiminishing production of such extensions surely indicates that the methods lack something.

The main reason for dissatisfaction with the Garrick method and other extensions of the Theodorsen method is simple. Even if airfoils were used of the same shape as are generally used as single airfoils,

the first transformation in the Garrick method gives a curve much less circle-like, especially for small spacing, than the corresponding transformation of Theodorsen for single airfoils - and as Theodorsen pointed out, nearness to a circle is important for minimizing the number of iterations necessary in the numerical process.

Numerical methods involving conformal transformation in which the final plane is not a single circle have also been devised. Mutterperl[32] transformed the arbitrary cascade into a flat plate cascade, for which the solution is well known. Shirakura[33] used four transformations to arrive at an annular region of flow, in which the airfoils have been transformed into both the inner and outer circles.

The simplest example of a numerical method in which the cascade is not conformally transformed into another figure is the "interference" method of Betz[34]. Here the properties of the isolated airfoil are assumed to be known (if not, they may be determined by Theodorsen's method) and the effect of the neighboring airfoils is assumed to be that of vortices, each placed at the location of another airfoil in the cascade. Betz outlined an iterative procedure which results finally in a distribution of singularities for each neighboring airfoil. Variations of this technique have been devised by Weinel[35], Katzoff et al[36], Woolard[37], Hutton[38], and others. The fact that these methods also become more cumbersome and less accurate as airfoil spacing decreases suggests that the difficulties of the previously described methods still have not been entirely eliminated.

One technique has been used which does become more simple and accurate as airfoil spacing decreases. This is the "stream

filament" method which is based on the older channel theory of steam turbines (reference 39, p. 992). If the airfoil spacing is sufficiently small, approximate streamlines and potential lines of the flow between the airfoils can easily be sketched freehand. Then from continuity considerations and an assumption as to the variation of velocity across the channel, the velocity on the airfoils may be determined. Huppert and MacGregor[40] have outlined such a procedure based upon linear variation of streamline curvature along potential lines. These methods are quite useful for spacing less than about half the chord, but are too inaccurate for most practical cascades. Finally there is the disadvantage that the velocity cannot be obtained for portions of the airfoil near the leading and trailing edges, especially for large stagger.

Summarizing, one may state that two general methods of approach to the arbitrary cascade problem have been used: In one case the Birnbaum model is used in a theory leading to equations giving flow characteristics in terms of cascade parameters. In the other case some kind of numerical method is devised, which must be applied to each cascade individually.

C. Rannie's Method and its Extension to the Cascade

Generally speaking, analytical methods have the advantage of giving greater insight into a solution than numerical methods, but it was pointed out above that results from the available thin airfoil theories can be considerably in error if the deviation of the airfoil from a flat plate is large. The flow characteristics which are particularly sensitive in this respect are velocity and pressure distribution, which are known to be given incorrectly near the leading edge in certain cases

by the foregoing thin airfoil theories. The importance of boundary layers in turbomachines and the intimate connection between boundary layer characteristics and pressure distribution provide the incentive for devising an analytic cascade theory which predicts realistic pressure distributions.

Following the example of Goldstein, who devised an analytic approximation to Theodorsen's method for single airfoils, W. D. Rannie has recently envisaged a similar approach to the Garrick method. His initial work (unpublished) was restricted to the single zero-thickness airfoil. Rannie was unable to discard the assumption of small camber, but departed from the Goldstein approach as follows: Goldstein utilized the smallness of certain quantities in the near-circle plane, while Rannie chose not to consider this plane, realizing that Goldstein's assumptions would not be as good for a cascade. Instead he assumed that the physical plane and the final circle plane could be related through a single transformation equation which could be determined. Rannie found the proper form of the overall transformation equation by combining the successive transformations (Equations 1 and 3) into a single equation and grouping unknown constants.

Rannie's equation for the overall transformation from the physical plane of a single airfoil to the circle plane is

$$w(z) = x(r,\phi) + i\,y(r,\phi) = \frac{1}{4}\left(z + \frac{1}{z}\right)(1+\Delta) + \sum_{n=0}^{\infty} \frac{B_n}{z^n} \qquad (7)$$

where Δ and the B_n must be determined. Applying this equation to zero-thickness parabolic and S-shaped airfoils, Rannie found that Δ and the B_n could be evaluated quite simply if they were assumed to be given

by power series in a linearization parameter. Substitution of x and y from Equation (7) into the equation of the airfoil shape, and equating coefficients of like powers of the linearization parameter led to simple equations for the unknown coefficients.

Though Rannie was unable to include the important effect of airfoil thickness in his theory, there was still an important improvement over the work of Birnbaum and Glauert. Rannie was able to find approximations of higher order than the first approximation which results from the earlier theory. The determination of first-order accuracy, for which the higher order terms are useful, provided an incentive for an extension to cascades of the work of Rannie plus the addition of the effect of thickness.

At the suggestion of Dr. Rannie, the author has attempted the extension of this work to the cascade problem. As might have been expected, the extension presented considerable difficulty. It was the original intention to follow Rannie's example and simply combine the successive transformations of the Garrick method, grouping unknown constants. Actually it was found that this approach was completely impractical for several reasons. For example it was found that the "additive function", $\sum \frac{B_n}{z^n}$, in Equation (7) is rapidly convergent compared to a similar series for a cascade, and it was found necessary to replace the series by an (initially unknown) function in closed form. The unknown function was determined by an auxiliary boundary value problem, for which a new method of solution was devised. This and other considerations (which will be omitted here) finally led to a form for the assumed overall cascade transformation equation which could

not have been obtained by the obvious extension of the work of Rannie, as first attempted.

In the following section the present theory will be presented for cascades with airfoils of the following shapes: (1) zero-thickness circular arc, (2) zero-thickness symmetric parabola, (3) zero-thickness S-shape, (4) symmetric airfoil with arbitrary thickness distribution, and (5) combinations of the previous shapes. Strictly speaking, the last and most general of these is not an arbitrary airfoil, but it is considered to be sufficiently general for most practical uses.

Following the analysis a section will be found devoted to a comparison with the results of previous investigations mentioned in this Introduction. A final section contains a discussion of the present results, including an error analysis.

II. ANALYSIS

As mentioned in the Introduction, in the method of solution used here a conformal transformation of the airfoils of the cascade into a unit circle is effected. Before the complicated details of this transformation are presented below, there will be found discussion of what is actually the final part of the problem - namely, the solution of the equivalent flow problem in the circle plane, plus interpretation in the physical plane.

Notation is listed in Appendix A.

A. The Solution of the Flow Problem

The $w = x + iy$ plane has already been selected as the physical plane - that is, the plane of the airfoils, and the $z = re^{i\phi}$ plane as the circle plane. Figure 3a shows the assumed orientation in the w plane of a cascade with stagger angle β and spacing-chord ratio σ. One airfoil has its downstream end, or trailing edge, at the point $w = \frac{1}{2}$ and its upstream end, or leading edge, at the point $w = -\frac{1}{2}$. Corresponding points on all the airfoils in the w plane are represented by a single point on the unit circle with center at the origin of the z plane (Figure 3b). For example the trailing edges labeled T in Figure 3a are represented by the point τ on the circle in Figure 3b. The argument (value of ϕ) of the point τ is ψ and is called the trailing edge argument (not to be confused with the trailing edge angle of an airfoil with a sharp trailing edge). Similarly the leading edges L are represented by the point λ whose argument is χ. The region outside the airfoils is transformed into the region exterior to the circle. In particular the point at infinity to the right of the cascade in the w plane

corresponds to the point $z = +\frac{1}{b}$, where b is a real number less than unity. The point $z = -\frac{1}{b}$ and the point at infinity to the left of the cascade in the w plane similarly correspond.

It has been assumed above that the transformation from the arbitrary airfoil of Figure 3a to the circle plane of Figure 3b is possible. The details of the transformation depend upon the cascade geometry, and will be discussed later in this section on Analysis. For the moment attention is directed only to the fact that though the values of quantities like b and ψ depend upon the original cascade geometry, the general appearance of the circle plane is the same for all cascades.

The flow in the physical plane w originates as a uniform flow of specified direction far to the left of the cascade. The fluid is deflected by the cascade, eventually becoming another uniform flow (with, in general, a new direction) far to the right of the cascade. The velocity vector diagram is shown in Figure 3c. The vectors V_U and V_D are the upstream and downstream vectors respectively. The vector V_∞ is the average of V_U and V_D, and is commonly employed in the analysis of cascades because of the property that the force on an airfoil is perpendicular to V_∞, similar to the case of a single airfoil. The angle of attack α gives the direction of this vector with respect to the airfoil chord line.

The corresponding flow in the circle plane is that from a source-vortex at $z = -\frac{1}{b}$, around the circle to a sink-vortex at $z = \frac{1}{b}$. The complex velocity potential P(z) can be shown to be given by

$$P(z) = \frac{\sigma}{\pi} V_\infty \left[e^{i\gamma} \tanh^{-1}\left(\frac{b}{z}\right) + e^{-i\gamma} \tanh^{-1}(bz) \right] + \frac{i\Gamma}{4\pi} \log \frac{(z+b)(z-b)}{(z+\frac{1}{b})(z-\frac{1}{b})} \qquad (8)$$

where Γ is the circulation about one airfoil, and $\gamma = \alpha + \beta$.

The circulation Γ in Equation (8) can be established by the Kutta condition, which states that the flow velocity must be finite at a sharp trailing edge. Stated mathematically,

$$\frac{\partial}{\partial \phi}\left[R\ell\ P(e^{i\psi}) \right] = 0. \tag{9}$$

If the trailing edge is not sharp, but rounded, the Kutta condition has no meaning. In this thesis Equation (9) shall be used to fix the circulation anyway; it must be borne in mind that for the airfoil with rounded trailing edge, this is arbitrary.

If Equation (8) is substituted into Equation (9), the resulting equation for circulation is

$$\Gamma = 4b\sigma V_\infty \left(\frac{\sin\gamma\cos\psi}{1+b^2} - \frac{\cos\gamma\sin\psi}{1-b^2} \right). \tag{10}$$

Equation (10) gives one of the flow characteristics (see Introduction) in terms of three cascade parameters (σ, γ, and V_∞) and two parameters from the circle plane (b and ψ). Hence if b and ψ are determined from the properties of the conformal transformation, the equation can be used to evaluate Γ. Similar equations will now be found for other flow characteristics.

The coefficient of lift, a quantity frequently used in aeronautics, is defined by the equation

$$C_L = \frac{\text{force exerted on an airfoil by the flow}}{\frac{1}{2}\rho V_\infty^2} \tag{11}$$

where ρ is the fluid density. It can be shown (see reference 1, p. 5) that the numerator of Equation (11) is equal to $\rho V \Gamma$ for a cascade.

Thus

$$C_L = \frac{2\Gamma}{V_\infty} \tag{12}$$

and from Equation (10)

$$C_L = 8b\sigma\left[\left(\frac{\cos\beta\cos\psi}{1+b^2} + \frac{\sin\beta\sin\psi}{1-b^2}\right)\sin\alpha + \left(\frac{\sin\beta\cos\psi}{1+b^2} - \frac{\cos\beta\sin\psi}{1-b^2}\right)\cos\alpha\right]. \tag{13}$$

Because its value depends greatly on upstream flow direction, the lift coefficient is less convenient to use in the design of axial flow compressors than a quantity called deviation angle, which may be defined as the angle between the downstream flow direction and the direction of a line tangent to the airfoil camber line at the trailing edge. The angle is illustrated in Figure 4, from which

$$\delta = \gamma_D - \beta + \vartheta_T . \tag{14}$$

An expression for δ similar to Equations (10) and (13) is

$$\delta = \tan^{-1}\left\{\frac{\frac{4b}{1-b^2}\sin\psi + \left(1 - \frac{2b}{1+b^2}\cos\psi\right)\tan\gamma_U}{1 + \frac{2b}{1+b^2}\cos\psi}\right\} - \beta + \vartheta_T \tag{15}$$

Another quantity which gives the downstream flow direction is the angle γ_D. Using Equations (14) and (15) gives

$$\tan\gamma_D = \frac{\frac{4b}{1-b^2}\sin\psi}{1 + \frac{2b}{1+b^2}\cos\psi} + \frac{1 - \frac{2b}{1+b^2}\cos\psi}{1 + \frac{2b}{1+b^2}\cos\psi}\tan\gamma_U \tag{16}$$

which shows that for a given cascade geometry there is a linear relationship between the tangents of the upstream and downstream flow angles.

The final overall flow characteristic to be considered here is the turning angle $\Omega = \gamma_U - \gamma_D$, which is given by

$$\Omega = \gamma_U - \tan^{-1}\left\{ \frac{\frac{4b}{1-b^2}\sin\psi + \left(1 - \frac{2b}{1+b^2}\cos\psi\right)\tan\gamma_U}{1 + \frac{2b}{1+b^2}\cos\psi} \right\}. \tag{17}$$

It was stated in the Introduction that the overall flow characteristics (such as Γ, C_L, δ, Ω) are essentially equivalent. This is illustrated by the equations just obtained, since all are dependent upon the same parameters. The velocity and pressure distributions require additional variables, however, and will now be obtained.

The complex velocity (a vector conjugate to the velocity vector) is given in the z plane by

$$\text{complex velocity in z plane} = \frac{d}{dz} P(z) = P'(z). \tag{18}$$

The corresponding complex velocity in the physical plane may be obtained from this expression and the transformation equation through

$$\text{complex velocity in w plane} = \frac{P'(z)}{w'(z)} \tag{19}$$

which indicates the importance of the transformation equation $w = w(z)$. When $z = e^{i\phi}$, the modulus of this expression is the velocity distribution V. Using Equation (8), the velocity distribution is

$$\frac{V}{V_\infty} = \left| \frac{2\frac{\sigma}{\pi}\frac{b}{1+b^4-2b^2\cos 2\phi}\left[(1+b^2)(\sin\phi-\sin\psi)\cos\gamma - (1-b^2)(\cos\phi-\cos\psi)\sin\gamma\right]}{w'(e^{i\phi})} \right| \tag{20}$$

Finally using the Bernoulli relationship between velocity and pressure, the pressure distribution is obtained as

$$\frac{P - P_\infty}{\frac{1}{2}\rho V_\infty^2} = 1 - \left(\frac{V}{V_\infty}\right)^2. \tag{21}$$

Equations (20) and (21) give velocity and pressure distribution in terms of ϕ, whereas it is usually desirable to know its variation with x, the position along the chord line. The required relation between x and ϕ must come from the transformation equation using

$$x = Re\left[w\left(e^{i\phi}\right)\right]. \tag{22}$$

From the foregoing it is apparent that for any given cascade geometry, certain details of the conformal transformation relating the cascade plane and the circle plane are required. In particular the quantities b and ψ are needed to find the overall flow characteristics. Furthermore the transformation equation must be determined if the velocity distribution is desired. Actually in the method used here b and ψ are found with the transformation equation; hence determination of the equation is the principal object of the analysis.

B. Technique for Determining the Conformal Transformation

The known exact solution to the flat plate cascade problem is the starting point of the present solution for the arbitrary cascade. The transformation equation for this special case, Equation (4), is repeated below in slightly different form:

$$w(z) = F_o(z) + \bar{F}_o\left(\frac{1}{z}\right) \tag{23}$$

where

$$F_o(z) = u_o(r,\phi) + i v_o(r,\phi) = \frac{\sigma}{\pi} e^{i\beta} \tanh^{-1}\left(\frac{b_o}{z}\right) \tag{24}$$

and $\overline{F}_0\left(\frac{1}{z}\right)$ is the conjugate complex function (see reference 12, p. 119) of $F_0(z)$. As shown in Figure 2b, the trailing edge argument is called ψ_0, the leading edge argument is χ_0, and the value of b is b_0. The trailing edges T and the leading edges L are represented on the circle by the points t and ℓ respectively, and are shown located diametrically opposite each other as dictated by symmetry considerations. The quantities σ, β, and b_0, are related through Equation (5). If Equation (23) is used to find the trailing edge argument ψ_0, the result may be expressed in the form

$$\tan \psi_0 = \frac{1-b_0^2}{1+b_0^2} \tan \beta . \tag{25}$$

Further details on this special case may be obtained from references 1, 5 or 14.

The arbitrary cascade shown in Figure 3a is assumed to consist of airfoils whose shape represents a small perturbation about a straight line. The equation for the shape of the particular airfoil located near the origin of the $w = x + iy$ plane of Figure 3a is assumed to have the form

$$y = y(x, \eta) \qquad \left(-\tfrac{1}{2} \le x \le \tfrac{1}{2}\right) \tag{26}$$

where η is a parameter expressing the deviation from the straight line; that is,

$$y(x, 0) = 0 \qquad \left(-\tfrac{1}{2} \le x \le \tfrac{1}{2}\right) \tag{27}$$

The parameter η can have simple physical significance, as will be shown later by examples. The further assumption is made that Equation (26) can be expanded in a power series of the form

$$y = \sum_{n=1}^{\infty} \eta^n g_n(x) \qquad \left(-\tfrac{1}{2} \le x \le \tfrac{1}{2}\right). \tag{28}$$

Then the first-order (or linearized) form of Equation (26) is

$$y = \eta\, g_1(x). \tag{29}$$

The qualification $-\frac{1}{2} \le x \le \frac{1}{2}$ has been omitted for brevity in Equation (29), but will be assumed here to apply to all equations of airfoil shape.

Equation (29) is the form in which the airfoil shape equation will be used most frequently in this thesis. Hence η will be assumed to be small. The function $g_1(x)$ is single valued when the airfoils have zero thickness and double valued otherwise. Since the leading and trailing edges are at the points $w = -\frac{1}{2}$ and $w = \frac{1}{2}$ respectively, it follows that

$$g_1\left(-\tfrac{1}{2}\right) = g_1\left(\tfrac{1}{2}\right) = 0. \tag{30}$$

Certain mathematical conditions are imposed on the transformation equation, $w = w(z)$. They are:

(1) $w(z)$ must be a regular function of z in the region $|z| \ge 1.0$, except for two singular points which correspond to the points far upstream and downstream of the cascade.

(2) $w(z)$ must be periodic of period $e^{i\left(\frac{\pi}{2} - \beta\right)}$.

(3) $w(e^{i\phi})$ must correspond to the closed figure described by Equation (26).

The basic technique used here for the determination of the transformation equation consists of two parts:

(1) Establishing a suitable form for the equation involving initially unknown functions and constants.

(2) Determining the functions and constants from the conditions imposed on the transformation equations.

In the first part of the technique the transformation equation must be obtained by suitably generalizing Equation (23). As mentioned in the Introduction, an extensive preliminary study led to the adoption of the following form:

$$w(z) = F(z) + \bar{F}\left(\frac{1}{z}\right) + \sum_{n=1}^{\infty} \eta^n F_n(z) \tag{31}$$

where

$$F(z) = u(r,\phi) + iv(r,\phi) = \frac{\sigma}{\pi} e^{i\beta} \tanh^{-1}\left(\frac{b}{z}\right) \tag{32}$$

$$b = b_0 + \sum_{n=1}^{\infty} \eta^n b_n \tag{33}$$

and the functions $F_n(z) = u_n(r, \phi) + iv_n(r, \phi)$ are regular in the region $|z| \geq 1.0$, including the point at infinity.

The first two of the three mathematical conditions imposed on w(z) are obviously satisfied in the same way as in Equation (23). The initially unknown functions $F_n(z)$ and constants b_n are determined by the third condition, through the equation of the airfoil shape, Equation (26). In addition Equation (26) can be used to find the trailing edge argument ψ and the leading edge argument χ, which are assumed to have the forms

$$\psi = \psi_0 + \sum_{n=1}^{\infty} \eta^n \psi_n \tag{34}$$

$$\chi = \pi + \psi_0 + \sum_{n=1}^{\infty} \eta^n \chi_n \tag{35}$$

where the constants ψ_n and χ_n are initially unknown.

It will be seen that the first-order quantities $F_1(z)$, b_1, ψ_1, and χ_1, must be found before the higher order terms can be evaluated. Hence terms of order η^2 and higher will be neglected initially. For example the first-order equation for b is

$$b = b_0 + \eta b_1 . \tag{36}$$

Taking real and imaginary parts of Equation (31) gives, after some manipulation

$$x(r,\phi) = 2u_0(r,\phi) + \eta\left[u_1(r,\phi) - 2\frac{b_1}{b_0}\frac{\partial}{\partial\phi}v_0(r,\phi)\right] \tag{37}$$

$$y(r,\phi) = \eta v_1(r,\phi) . \tag{38}$$

These are to be considered now for r = 1. Adopting the notation

$$\begin{aligned} x &= x(1,\phi) & u_0' &= \frac{\partial}{\partial\phi}u_0(1,\phi) \\ u_0 &= u_0(1,\phi) & v_1' &= \frac{\partial}{\partial\phi}v_1(1,\phi) \\ &\cdots & &\cdots \end{aligned} \tag{39}$$

makes it possible to write Equations (37) and (38) (with r = 1) in shorter form:

$$x = 2u_0 + \eta(u_1 - 2\frac{b_1}{b_0}v_0') \tag{40}$$

$$y = \eta v_1 . \tag{41}$$

Since these refer to the unit circle in the z plane, they can be substituted into Equation (29), leading to

$$v_1 = g_1(2u_0) . \tag{42}$$

Thus an expression has been obtained for the imaginary part (on the unit circle) of the initially unknown function $F_1(z)$. Determination of $F_1(z)$ from this information is a standard mathematical problem, which herein shall be called the auxiliary boundary value problem, or for convenience, simply "BVP". A special technique for solving the BVP was devised here and is illustrated for a particular case in Appendix B. The solution of the BVP involves an arbitrary real constant which for convenience is established by the following final condition to be met by the BVP solution:

$$u_{1t} + u_{1\ell} = 0 \tag{43}$$

where the subscripts t and ℓ signify evaluation at the values of ϕ corresponding to the points t and ℓ on the unit circle of Figure 2b. That is,

$$u_{1t} = u_1(1, \psi_0) \tag{44}$$

$$u_{1\ell} = u_1(1, \alpha_0) = u_1(1, \pi + \psi_0). \tag{45}$$

Since $F_1(z)$ can now be considered as known, the evaluation of b_1 will complete the determination of the first order transformation equation. Equation (40) can be used for this purpose. It should be emphasized that Equation (40) is an equation for x in terms of independent argument ϕ, selection of which determines a point on the unit circle in the z plane. Evaluation at the point τ gives

$$x_\tau = 2u_{0t} + \eta\left(u_{1\tau} - 2\frac{b_1}{b_0}v'_{0\tau}\right). \tag{46}$$

Since τ is the point on the circle corresponding to the trailing edges T, x_τ must be unity. Equation (46) could now be used to evaluate b_1

except that the trailing edge argument ψ is not known, hence $u_{o\tau}$, $u_{1\tau}$, and $v'_{o\tau}$ cannot be determined. However these can be evaluated by means of Taylor's theorem. For instance

$$u_{o\tau} = u_{ot} + (\psi - \psi_0) u'_{ot} + \cdots = u_{ot} + \eta \psi_1 u'_{ot} \tag{47}$$

with similar expressions for $u_{1\tau}$ and $v'_{o\tau}$. Thus Equation (46) can be written

$$x_\tau = 2u_{ot} + \eta \left(u_{1t} - 2 \frac{b_1}{b_0} v'_{ot} + 2\psi_1 u'_{ot} \right). \tag{48}$$

In a similar manner one can find x_λ in the form

$$x_\lambda = 2u_{ol} + \eta \left(u_{1l} - 2 \frac{b_1}{b_0} v'_{ol} + 2 \chi_1 u'_{ol} \right). \tag{49}$$

From Equation (24) one can show that

$$u_{ot} = \tfrac{1}{4} = - u_{ol} \tag{50}$$

$$u'_{ot} = 0 = u'_{ol} \tag{51}$$

$$u''_{ot} = - u''_{ol} \tag{52}$$

$$v'_{ot} = -v'_{ol} \neq 0 \tag{53}$$

$$v''_{ot} = - v''_{ol} \ . \tag{54}$$

Furthermore it is obvious from Figure 3 that

$$x_\tau = \tfrac{1}{2} = - x_\lambda \tag{55}$$

$$x'_\tau = 0 = x'_\lambda \ . \tag{56}$$

Substitution of Equations (43), (50), (51), (53), and (55) into either Equation (48) or (49) leads to an equation for b_1, namely:

$$b_1 = \frac{b_0 u_{1t}}{2 v'_{ot}} \tag{57}$$

The first-order transformation equation is now complete, but the constants ψ_1 and χ_1 are yet to be found. Differentiation with respect to ϕ of Equations (48) and (49) gives, using Equation (57),

$$x'_\tau = 2u'_{ot} + \eta\left(u'_{1t} - \frac{u_{1t}}{v'_{ot}} v''_{ot} + 2\psi_1 u''_{ot}\right) \tag{58}$$

$$x'_\lambda = 2u'_{ol} + \eta\left(u'_{1l} - \frac{u_{1t}}{v'_{ot}} v''_{ol} + 2\chi_1 u''_{ol}\right). \tag{59}$$

Substitutions similar to those used in the equations for x_τ and x_λ lead to

$$\psi_1 = \frac{u_{1t} v''_{ot}}{2u''_{ot} v'_{ot}} - \frac{u'_{1t}}{2u''_{ot}} \tag{60}$$

$$\chi_1 = \frac{u_{1t} v''_{ot}}{2u''_{ot} v'_{ot}} + \frac{u'_{1l}}{2u''_{ot}} . \tag{61}$$

This completes the analysis of the first order transformation properties.

Higher order terms in the transformation equation can also be obtained in the same way. The procedure for second order terms will be briefly outlined. Equations for x and y are again written, this time including terms of order η^2:

$$x = 2u_0 + \eta\left(u_1 - 2\frac{b_1}{b_0} v_0'\right) + \eta^2\left(u_2 - 2\frac{b_2}{b_0} v_0' + b_1^2 \mathrm{Rl}\, F_0''\right) \tag{62}$$

$$y = \eta v_1 + \eta^2 v_2 . \tag{63}$$

Substitution into Equation (28) leads to the following second order BVP: Find $F_2(z)$ if

$$v_2 = \left(u_1 - z\frac{b_1}{b_0} v_0'\right) \frac{d}{dx} g_1(2u_0) + g_2(2u_0) \tag{64}$$

$$u_{2t} + u_{2\ell} = 0. \tag{65}$$

Then evaluation of x_τ, x_λ, x'_τ, and x'_λ leads to equations for b_2, ψ_2, and χ_2, namely

$$b_2 = \frac{b_0 u_{2t}}{2v'_{ot}} - \frac{b_0 u''_{ot}}{2v'_{ot}} \psi_1^2 + \frac{b_0 b_1^2}{2v'_{ot}} Rl\, F''_{ot} \tag{66}$$

$$\psi_2 = \frac{b_2}{b_0}\frac{v''_{ot}}{u''_{ot}} - \psi_1^2\left(\frac{u'''_{ot}}{2u''_{ot}} - 1\right) - \frac{b_1^2}{2u''_{ot}}\left(Rl\, F''_{ot}\right)' - \frac{u'_{2t}}{2u''_{ot}} + \frac{\psi_1}{2u''_{ot}}\left(u'_{1t} - u''_{1t}\right) \tag{67}$$

$$\chi_2 = \frac{b_2}{b_0}\frac{v''_{ot}}{u''_{ot}} - \chi_1^2\left(\frac{u'''_{ot}}{2u''_{ot}} - 1\right) - \frac{b_1^2}{2u''_{ot}}\left(Rl\, F''_{ot}\right)' + \frac{u'_{2\ell}}{2u''_{ot}} - \frac{\chi_1}{2u''_{ot}}\left(u'_{1\ell} - u''_{1\ell}\right) \tag{68}$$

provided that $\chi_1 = \pm \psi_1$.

The application of these equations to several cases will now be shown.

C. Cascade with Zero-Thickness Circular Arc Airfoils

In this case, which can also be called the "circular arc cascade", the airfoil coincides with its camber line. The camber angle is the angle between the tangents at the leading and trailing edges of one air-

foil. (A more general definition is given later when the S-shape angle is introduced). The equation of the circular arc airfoil with camber angle θ, located at the origin of the w plane is

$$y = -\tfrac{1}{2}\cot\tfrac{\theta}{2} + \sqrt{\tfrac{1}{4}\csc^2\tfrac{\theta}{2} - x^2}\,. \tag{69}$$

1. Characteristics of the Conformal Transformation

The linearization parameter η of the previous equations, can be conveniently taken here as θ, since $\theta = 0$ signifies a flat plate cascade. The power series expansion for Equation (69) is

$$y = \tfrac{1}{8}\theta(1-4x^2) + \mathcal{O}(\theta^3). \tag{70}$$

Since $\eta = \theta$ here it is evident from Equation (29) that

$$g_1^{(\theta)}(x) = \tfrac{1}{8}(1-4x^2) \tag{71}$$

where the superscript $(^{(\theta)})$ is used to distinguish this case from others to follow. The first-order BVP for this case can be solved by means of a special technique; details of the solution are given in Appendix B. The result is $F_1^{(\theta)}(z)$, which can be used in Equations (57) and (60) to find the following expressions for $b_1^{(\theta)}$ and $\psi_1^{(\theta)}$.

$$b_1^{(\theta)} = 0 \tag{72}$$

$$\psi_1^{(\theta)} = -\frac{\eta}{\pi}\,\frac{1-b_0^4}{b_0 Q}\tanh^{-1}(b_0^2). \tag{73}$$

Second-order terms will be discussed later.

2. Overall Flow Characteristics

The first two terms in the power series for b and ψ constitute first-order approximations to these quantities. Hence they

can now be computed and substituted into the previous equations for overall flow characteristics. An alternative procedure is to substitute $b = b_0 + \theta(\theta^2)$ and $\psi = \psi_0 + \theta\psi_1^{(\theta)} + \theta(\theta^2)$, and use Equations (25) and (73) to obtain the flow characteristics themselves in series form. Thus for lift coefficient we obtain, using Equation (13), and neglecting terms of order θ^2 and higher,

$$C_L = A_0 \sin\alpha + \theta\left(A_1^{(\theta)} \sin\alpha + B_1^{(\theta)} \cos\alpha\right) \tag{74}$$

where

$$A_0 = \frac{8 b_0 \sigma}{Q} \tag{75}$$

$$B_1^{(\theta)} = \frac{8\sigma^2}{\pi} \tanh^{-1}(b_0^2) \tag{76}$$

$$A_1^{(\theta)} = -\frac{1}{8}\left(\frac{A_0}{2\sigma}\right)^2 B_1 \sin 2\beta \tag{77}$$

From Equation (15),

$$\delta = \delta_0 + \theta\delta_1^{(\theta)} \tag{78}$$

where

$$\delta_0 = \tan^{-1}\left[\frac{\frac{4b_0}{Q}\sin\beta + \left(1 - \frac{2b_0}{Q}\cos\beta\right)\tan\gamma_U}{1 + \frac{2b_0}{Q}\cos\beta}\right] - \beta \tag{79}$$

$$\delta_1^{(\theta)} = \frac{1}{2} - \frac{\frac{(1+b_0^2)^2}{Q^2}\cos\beta + \frac{2b_0}{Q} + \frac{(1-b_0^2)^2}{Q^2}\sin\beta\tan\gamma_U}{\left(1 + \frac{2b_0}{Q}\cos\beta\right)^2 + \left[\frac{4b_0}{Q}\sin\beta + \left(1 - \frac{2b_0}{Q}\cos\beta\right)\tan\gamma_U\right]^2} \frac{4\sigma}{\pi}\tanh^{-1}(b_0^2). \tag{80}$$

And in place of Equation (16)

$$\tan \gamma_D = C + D \tan \gamma_U \tag{81}$$

where

$$C = C_0 + \theta C_1^{(\theta)} \tag{82}$$

$$D = D_0 + \theta D_1^{(\theta)} \tag{83}$$

$$C_0 = \frac{\frac{4b_0}{Q} \sin\beta}{1 + \frac{2b_0}{Q} \cos\beta} \tag{84}$$

$$D_0 = \frac{1 - \frac{2b_0}{Q} \cos\beta}{1 + \frac{2b_0}{Q} \cos\beta} \tag{85}$$

$$C_1^{(\theta)} = -\frac{4\frac{\sigma}{\pi}}{\left(1 + \frac{2b_0}{Q}\cos\beta\right)^2} \left[\frac{(1+b_0^2)^2}{Q^2} \cos\beta + \frac{2b_0}{Q} \right] \tanh^{-1}(b_0^2) \tag{86}$$

$$D_1^{(\theta)} = -\frac{4\frac{\Gamma}{\pi} \frac{(1-b_0^2)^2}{Q^2} \sin\beta}{\left(1 + \frac{2b_0}{Q}\cos\beta\right)^2} \tanh^{-1}(b_0^2). \tag{87}$$

In all of these equations σ, β, and b_0 are related through Equation (5). Similar expressions for Γ and Ω can also be found.

3. Approximate Formulas for Coefficients in the Equation for Deviation Angle

The formulas for the coefficients δ_0 and $\delta_1^{(\theta)}$ in Equation (78) are somewhat complicated in the exact forms given in Equations (79)

and (80). More convenient approximate expressions can be obtained in various ways. The method to be used here is to linearize the quantity b_0 about the points $b_0 = 1$ and $b_0 = 0$. This has an added advantage, it will be seen, of eliminating b_0 from the equations, leaving them entirely in terms of geometrical quantities. For example, if it is assumed that

$$b_0 = 1 - \Delta \tag{88}$$

and this is substituted into Equation (80), a power series in the quantity Δ is obtained:

$$\delta_1^{(\theta)} = \frac{1}{2} + \frac{\sigma}{\pi}\cos\beta\log\Delta + \Delta\frac{\sigma}{2\pi}\cos\beta + \Delta^2\frac{\sigma}{4\pi\cos\beta}\left(\log\Delta - \tfrac{1}{2}\cos^2\beta\right) + \theta(\Delta^3) \tag{89}$$

provided that $|\beta| \neq \frac{\pi}{2}$.

Next expressions must be found for Δ and $\log\Delta$ which involve only the geometrical parameters σ and β. If Equation (88) is substituted into Equation (5), the following equation is obtained:

$$\frac{\pi}{\sigma} = -2\cos\beta\log\Delta + 2\cos\beta\left(\log 2\cos\beta + \beta\tan\beta\right) - \Delta\cos\beta - \Delta^2\frac{1+\sin^2\beta}{4\cos\beta} + \theta(\Delta^3). \tag{90}$$

Thus

$$\log\Delta = -\frac{\pi}{2\sigma\cos\beta} + \log 2\cos\beta + \beta\tan\beta - \frac{\Delta}{2} - \Delta^2\frac{1+\sin^2\beta}{8\cos^2\beta} + \theta(\Delta^3) \tag{91}$$

from which

$$\Delta = 2\cos\beta\, e^{\beta\tan\beta - \frac{\pi}{2\sigma\cos\beta}} + \theta(\Delta^2). \tag{92}$$

Substitution of Equations (91) and (92) into Equation (89) gives

$$\delta_1^{(\theta)} = \frac{\sigma}{\pi}A\cos\beta - \epsilon\left(\frac{1}{2} + \frac{\sigma}{\pi}\cos\beta - \frac{\sigma}{\pi}A\cos\beta\right) + \theta(\epsilon^2) \tag{93}$$

where

$$A = \log 2\cos\beta + \beta\tan\beta \tag{94}$$

$$\epsilon = e^{2\beta\tan\beta - \frac{\pi}{\sigma\cos\beta}} \tag{95}$$

In a similar manner

$$\delta_0 = \epsilon\cos^2\beta\,(\tan\gamma_U - \tan\beta) + \theta(\epsilon^2). \tag{96}$$

Assuming that b_0 is a small quantity gives two more approximate equations for δ_0 and $\delta_1^{(\theta)}$:

$$\delta_0 = \alpha - \frac{\pi}{\sigma}\cos\beta\cos^2\gamma_U\,(\tan\gamma_U - \tan\beta) + \theta\left(\frac{1}{\sigma^3}\right) \tag{97}$$

$$\delta_1^{(\theta)} = \frac{1}{2} - \frac{\pi}{4\sigma}\cos\beta\cos^2\gamma_U\,(1 + \tan\beta\tan\gamma_U) + \theta\left(\frac{1}{\sigma^3}\right). \tag{98}$$

Equations (93) and (96) are easily recognized as being valid for σ small, while Equations (97) and (98) are valid for σ large. A partial check on the present theory is the agreement with the limiting values

$$\delta = 0 \qquad \text{when} \quad \sigma = 0 \text{ (infinite solidity cascade)} \tag{99}$$

$$\delta = \alpha + \frac{\theta}{2} \qquad \text{when} \quad \sigma = \infty \text{ (single airfoil).} \tag{100}$$

The exact equations for δ_0 and $\delta_1^{(\theta)}$ and the approximations for σ small, were plotted versus σ for various values of β and γ_U, to find the range of σ for which the approximate equations are reasonably accurate. The results indicate that Equations (93) and (96)

are quite good in the range $\sigma < 1.25$, except for stagger angle β near 90°, where the range is $\sigma < 1.00$. In mathematical language the restrictions on σ can be expressed as:

$$\sigma < 1.25 \quad \text{and} \quad \epsilon < 0.4 . \tag{101}$$

4. Terms of Higher Order in Camber Angle

The method used here is not limited to finding first-order terms in camber angle. Second-order and higher (nth-order) terms can also be found. The significance of the higher order terms in this analysis was discussed in Part I. Unfortunately the higher order expressions were found to be quite complicated, involving untabulated functions similar to those to be described presently in the treatment of S-shaped airfoils. Furthermore no general equations were found for nth-order terms. Instead each order had to be treated individually, with complexity increasing as the order increased.

The solution for the second-order auxiliary boundary value problem is

$$F_2^{(\theta)}(z) = -i F_0(z)\left[F_1^{(\theta)}(z) + \bar{F}_1^{(\theta)}\left(\tfrac{1}{z}\right)\right] - F_0(z)\,\bar{F}_0\left(\tfrac{1}{z}\right)\left[F_0(z) + \bar{F}_0\left(\tfrac{1}{z}\right)\right]$$

$$-\frac{\sigma^3}{\pi^3} b_0 \left[e^{-i\beta} z \int_0^{b_0^2} \frac{(\tanh^{-1}\xi)^2\, d\xi}{b_0^2 z^2 - \xi^2} + \frac{e^{i\beta}}{z} \int_0^{b_0^2} \frac{(\tanh^{-1}\xi)^2\, d\xi}{\frac{b_0^2}{z^2} - \xi^2} \right] \tag{102}$$

from which expressions for $b_2^{(\theta)}$, $\psi_2^{(\theta)}$, and $\chi_2^{(\theta)}$ can be found using equations given earlier. The results are much more involved than the equations for $b_1^{(\theta)}$, $\psi_1^{(\theta)}$, and $\chi_1^{(\theta)}$. It was found that some simplification could be obtained using the methods of the preceding section - i.e., if the range of σ were restricted. For example

the second-order coefficient in the following equation for deviation angle,

$$\delta = \delta_0 + \theta \delta_1^{(\theta)} + \theta^2 \delta_2^{(\theta)} \tag{103}$$

is $\delta_2^{(\theta)}$; for small σ the second-order theory indicates that it is given by

$$\delta_2^{(\theta)} = \frac{\sigma}{2\pi}\left(A \sin\beta - \frac{\beta}{\cos\beta}\right) - \frac{\sigma^2}{2\pi^2}\left(\beta \log\frac{\cos\beta}{2} - 2\int_0^\beta \log\cos\xi \, d\xi \right.$$

$$\left. - \beta A - A^2 \sin\beta \cos\beta\right) + \theta(\epsilon). \tag{104}$$

This is much more complex than the corresponding approximate equation for $\delta_1^{(\theta)}$, which from Equation (93) is

$$\delta_1^{(\theta)} = \frac{\sigma}{\pi} A \cos\beta + \theta(\epsilon). \tag{105}$$

If higher order terms are sufficiently large, computation of flow characteristics from first-order results will be in error. The magnitude of higher order terms in the deviation angle equation is determined by the values of θ, γ_U, σ, and β. A plot of higher order terms versus these four variables is obviously impractical, but considerable information can be gained from a plot of $\delta_2^{(\theta)}/\delta_1^{(\theta)}$, which eliminates the variable θ. Furthermore inspection of Equations (104) and (105) indicates that γ_U has no effect on $\delta_2^{(\theta)}$ or $\delta_1^{(\theta)}$ if σ is sufficiently small. The ratio $\delta_2^{(\theta)}/\delta_1^{(\theta)}$ is plotted in Figure 5 as a function of the remaining variables σ and β. Further reference is made to this figure in a subsequent section on error analysis.

5. Smooth Entry

The term smooth entry will be used to describe the flow condition such that the fluid enters the cascade smoothly at the leading edge

of each airfoil. It obviously has meaning only for zero-thickness airfoils. There is but one upstream flow direction for which the condition is attained.

In turbomachinery design, smooth entry is sometimes taken as design condition even for airfoils with thickness, by assuming for this purpose that the thickness is zero. In this case the flow angles and approximate spacing are given and the problem is to find the camber angle and blade setting for smooth entry.

Equation 69 indicates that a circular arc cascade which differs from another only in the sign of θ will coincide with the second if it is rotated about an appropriate axis perpendicular to the cascade plane. If the Kutta condition is applied simultaneously to the two cascades, the smooth entry condition must result. To arrive at equations valid for this condition, the expression for downstream flow angle is the most convenient to use. Equation (81) written for the two cascades is

$$\tan \gamma_D = C + D \tan \gamma_U \tag{106}$$

$$\tan \gamma_D' = C' + D' \tan \gamma_U' \tag{107}$$

where primed quantities refer to the second, or rotated cascade. At the smooth entry condition these must be simultaneous equations, and furthermore

$$\gamma_U' = \gamma_D \tag{108}$$

$$\gamma_D' = \gamma_U \tag{109}$$

so that Equation (107) can be written

$$\tan \gamma_U = c' + D' \tan \gamma_D . \tag{110}$$

Now Equations (106) and (110) can be solved for $\tan \gamma_U$ and $\tan \gamma_D$, from which can easily be found the turning angle Ω, given by

$$\Omega = \gamma_U - \gamma_D . \tag{111}$$

The result appears in the form

$$\Omega = \theta \Omega_1^{(\theta)} + \theta(\theta^3) \tag{112}$$

where

$$\Omega_1^{(\theta)} = \frac{4\sigma}{\pi} \cos\beta \tanh^{-1}(b_0^2). \tag{113}$$

The corresponding equation for stagger angle is

$$\beta = \beta_0 + \theta(\theta^2) \tag{114}$$

where

$$\beta_0 = \frac{\gamma_U + \gamma_D}{2} \tag{115}$$

Particularly simple first-order expressions can be obtained for velocity distribution and pressure distribution in the case of smooth entry. Use of the above results and Equations (20) and (21) leads to

$$\frac{V}{V_\infty} = 1 - \theta 2 v_0 \tag{116}$$

$$\frac{p - p_\infty}{\frac{1}{2}\rho V_\infty^2} = \theta 4 v_0 \tag{117}$$

where

$$v_0 = \frac{\sigma}{\pi} \operatorname{Im}\left[e^{i\beta} \tanh^{-1}(b_0 e^{-i\varphi}) \right]. \tag{118}$$

Finally use of Equation (22) leads to

$$x = 2u_o + \theta\left(2u_o v_o - 2u_{ot} v_{ot} - \frac{\sigma^2}{\pi^2} I + \frac{\sigma^2}{\pi^2} I_t\right) \tag{119}$$

where

$$u_o = \frac{\sigma}{\pi} Re\left[e^{i\beta} \tanh^{-1}(b_o e^{-i\phi})\right] \tag{120}$$

$$I = 2 b_o^2 \sin 2\phi \int_0^{b_o^2} \frac{\xi \tanh^{-1}\xi \, d\xi}{b_o^4 + \xi^4 - 2 b_o^2 \xi^2 \cos 2\phi} . \tag{121}$$

D. Cascade with Zero-Thickness Symmetric Parabolic Airfoils

The airfoil shape equation in this case is

$$y = \frac{1}{4}(1-4x^2)\tan\frac{\theta}{2} \tag{122}$$

and in series form is

$$y = \frac{1}{8}\theta(1-4x^2) + \theta(\theta^3) . \tag{123}$$

Comparison with Equation (70) indicates that this shape and the circular arc differ only in terms of order θ^3 at most. Hence the circular arc results in series form can also be used in this case up to terms of order θ^3.

E. Cascade with Zero-Thickness S-Shapted Airfoils

For this case the camber angle is zero and it is necessary to define a new parameter μ, called the S-shape angle. Figure 6 shows an arbitrary airfoil, and illustrates the angles ν_T and ν_L used in the following definition of μ:

$$\mu = \nu_T - \nu_L . \tag{124}$$

A similar definition for camber angle also involves ϑ_T and ϑ_L: the camber angle for the arbitrary airfoil of Figure 6 is

$$\theta = \vartheta_T + \vartheta_L . \tag{125}$$

The S-shaped airfoil is defined here as having the shape expressed by

$$y = \tfrac{1}{2} x (1-4x^2) \tan \tfrac{\mu}{2} . \tag{126}$$

Here $\vartheta_T = \tfrac{1}{2}\mu$ and $\vartheta_L = -\tfrac{1}{2}\mu$.

1. Characteristics of the Conformal Transformation

The first order transformation equation can be found as before by letting $\eta = \mu$. The solution of the auxiliary boundary value problem is

$$F_1^{(\mu)}(z) = 2F_0(z)\left[F_1^{(\theta)}(z) - \bar{F}_1^{(\theta)}(\tfrac{1}{z})\right] - 2i\,F_0(z)\,\bar{F}_0(\tfrac{1}{z})\left[F_0(z) - \bar{F}_0(\tfrac{1}{z})\right]$$

$$- 6i\frac{\pi^3}{\pi^3} b_0 \left[e^{-i\beta} z \int_0^{b_0^2} \frac{(\tanh^{-1}\xi)^2 d\xi}{b_0^2 z^2 - \xi^2} - \frac{e^{i\beta}}{z} \int_0^{b_0^2} \frac{(\tanh^{-1}\xi)^2 d\xi}{\frac{b_0^2}{z^2} - \xi^2} \right] \tag{127}$$

which can be used with previous equations to find b and ψ.

2. Complexity of the Results

It is possible to write exact expressions for the coefficients of μ in equations (in series form) for overall flow characteristics as was done for the circular arc cascade. However the exact expressions contain integrals which cannot be expressed in terms of the same functions as before. One can express some of the integrals in terms of either of two known transcendental functions, called the dilogarithm (see reference 41, p. 31, or reference 42) and Spence's Integral[43],

but these functions are required for complex arguments and are not tabulated in the literature except for real arguments[44]. Thus the exact equations in terms of these functions will not be useful until they are tabulated completely and will not be given here.

Fortunately approximate expressions for coefficients of μ (derived from the exact equations by the same methods used for the circular arc cascade) are in terms of simple functions. Hence in what follows the approximate expressions will be given.

3. Deviation Angle

The equation for deviation angle, obtained in the same way as was used for the circular arc cascade, is

$$\delta = \delta_0 + \mu \delta_1^{(\mu)} + \theta(\mu^2) \tag{128}$$

where δ_0 is already known and if σ is small,

$$\begin{aligned}\delta_1^{(\mu)} = {} & \frac{3\sigma}{\pi} A \cos\beta - \frac{3\sigma^2}{\pi^2}\left(\frac{\pi^2}{12} + A^2\cos^2\beta\right) \\ & + \epsilon\left\{\frac{1}{2} + \frac{3\sigma}{\pi}\cos\beta - \frac{3\sigma}{\pi} A\cos\beta + \frac{6\sigma^2}{\pi^2}\left[\frac{1}{2}\left(\frac{\pi^2}{12} + A^2\cos^2\beta\right)\right.\right. \\ & \left. -2\log 2\cos\beta + (1 + \log 2\cos\beta - \beta\tan\beta)\cos^2\beta\right] \\ & - (\tan\gamma_0 - \tan\beta)\left[\beta - 3\tan\beta\log 2\cos\beta + \frac{6\sigma}{\pi}(A^2 - \beta^2)\sin\beta\right. \\ & \left.\left. + \frac{4\sigma^2}{\pi^2}\left(\frac{\beta^3}{\cos^2\beta} - A^3\tan\beta\cos^2\beta\right)\right]\right\} + \theta(\epsilon^2).\end{aligned} \tag{129}$$

Here A and ϵ are again given by Equations (94) and (95). One may reasonably expect Equation (129) to be sufficiently accurate for $\sigma < 1.25$, $\epsilon < 0.4$, as for the circular arc cascade.

4. Smooth Entry

The two equations for smooth entry corresponding to Equations (112) and (114) are

$$\Omega = \theta(\mu^2) \tag{130}$$

$$\beta = \beta_0 + \mu \beta_1^{(\mu)} + \theta(\mu^2) \tag{131}$$

where β_0 is already known and for $\sigma < 1.25$, $\epsilon < 0.4$,

$$\beta_1^{(\mu)} = \frac{1}{2} - \frac{3\sigma}{\pi} A \cos\beta + \frac{3\sigma^2}{\pi^2}\left(\frac{\pi^2}{12} + A^2\cos^2\beta\right)$$

$$-\epsilon\left[\frac{3\sigma}{\pi} A\cos\beta + \frac{6\sigma^2}{\pi^2}\left(\cos^2\beta - A\cos^2\beta - 2\sin^2\beta \log_e 2\cos\beta\right)\right] + \theta(\epsilon^2). \tag{132}$$

F. Cascade with Symmetric Airfoils of Arbitrary Thickness Distribution

In this case the equation of the airfoil is

$$y = \pm \tau f(x) \tag{133}$$

where the $\pm$ sign refers to the two surfaces of the airfoil (usually called upper and lower surfaces) and τ is the maximum thickness expressed as a fraction of the chord. Thus the arbitrary thickness function f(x) has a maximum value of 0.5.

1. Characteristics of the Conformal Transformation

The treatment here resembles that of the previous cases with $\eta = \tau$ and $g_1^{(\tau)}(x) = \pm f(x)$. However the resulting auxiliary boundary value problem (BVP) does not lend itself to the method of Appendix B, because of the more general form of Equation (133). Instead the BVP must be solved by one of the Poisson formulas. Since in most cases the function sought is to be evaluated only on the unit circle, the

problem is one of conjugation and the techniques developed for the Theodorsen method for single airfoils can be used[11], [23], [24]. The advantages of the present theory are: (1) no iteration is required, and (2) one conjugation suffices for all values of maximum thickness (which of course is assumed to be small).

The BVP statement itself is: Find $F_1^{(\tau)}(z) = u_1^{(\tau)}(r,\phi) + iv_1^{(\tau)}(r,\phi)$, regular everywhere in $|z| \geq 1$, if $v_1^{(\tau)} = \pm f(2u_0)$ and $u_{1t}^{(\tau)} + u_{1l}^{(\tau)} = 0$. The plus sign applies to the range $\psi_0 \leq \phi \leq \psi + \pi$ and the minus sign elsewhere.

G. Cascade with Airfoils Derived From Combinations of the Previous Cases

This is the most general case considered here and is sufficiently arbitrary for most practical purposes. For example consider an airfoil of maximum thickness τ with a cubic camber line of camber angle θ and S-shape angle μ. Assuming the thickness is measured normal to the chord line and is a function of position on the chord line, the equation of the airfoil is

$$y = \frac{1}{8}(1-4x^2)\left[\tan\left(\frac{\theta}{2}+\frac{\mu}{2}\right)+\tan\left(\frac{\theta}{2}-\frac{\mu}{2}\right)\right]$$
$$+\frac{1}{4}x(1-4x^2)\left[\tan\left(\frac{\theta}{2}+\frac{\mu}{2}\right)-\tan\left(\frac{\theta}{2}-\frac{\mu}{2}\right)\right] \pm \tau f(x). \qquad (134)$$

It is obvious that the exact form of the airfoil equation can be quite complicated, depending upon the method of construction (see Introduction).

Fortunately the first-order equation for any combination of the four previous cases has a simple form regardless of the method of adding thickness, because the differences are of second order. In general this equation is

$$y = \frac{1}{8}\theta(1-4x^2) + \frac{1}{4}\mu x(1-4x^2) \pm \tau f(x) . \tag{135}$$

1. Overall Flow Characteristics

The principle of superposition of linearized solutions makes it possible to immediately write expressions for various quantities. For example the first approximations for b and ψ are

$$b = b_0 + \theta b_1^{(\theta)} + \mu b_1^{(\mu)} + \tau b_1^{(\tau)} \tag{136}$$

$$\psi = \psi_0 + \theta \psi_1^{(\theta)} + \mu \psi_1^{(\mu)} + \tau \psi_1^{(\tau)} \tag{137}$$

where the coefficients of θ, μ, and τ have already been given. These equations can be used in Equations (10), (13), (15), (16), and (17) to find the various overall flow characteristics.

2. Velocity and Pressure Distribution

Without higher order terms the transformation equation for this case is

$$w(z) = F(z) + \bar{F}\left(\frac{1}{z}\right) + \theta F_1^{(\theta)}(z) + \mu F_1^{(\mu)}(z) + \tau F_1^{(\tau)}(z) . \tag{138}$$

Substitution into Equation (20) yields the velocity distribution

$$\frac{V}{V_\infty} = \left| \frac{\frac{2\sigma}{\pi} b \frac{(1+b^2)(\sin\phi - \sin\psi)\cos\gamma - (1-b^2)(\cos\phi - \cos\psi)\sin\gamma}{1+b^4-2b^2\cos 2\phi}}{\left\{\left[\frac{2\sigma}{\pi} b \frac{(1-b^2)\sin\beta\cos\phi - (1+b^2)\cos\beta\sin\phi}{1+b^4-2b^2\cos 2\phi} + \theta u_1^{(\theta)'} + \mu u_1^{(\mu)'} + \tau u_1^{(\tau)'}\right]^2 + \left[\theta v_1^{(\theta)'} + \mu v_1^{(\mu)'} + \tau v_1^{(\tau)'}\right]^2\right\}^{\frac{1}{2}}} \right| \tag{139}$$

Using Equation (22) gives the auxiliary relation between x and ϕ :

$$x = \frac{2\sigma}{\pi} \mathrm{Re}\left[e^{i\beta} \tanh^{-1}(b_0 e^{-i\phi})\right] + \theta u_1^{(\theta)} + \mu u_1^{(\mu)} + \tau u_1^{(\tau)} \tag{140}$$

The pressure distribution may be obtained using Equation (21).

III. COMPARISON WITH PREVIOUS INVESTIGATIONS

In this section results are compared with the work of some of the authors mentioned in the Introduction. Notation of this thesis is used throughout for convenience.

A. Lift Coefficient

The following equation for lift coefficient was obtained by Klingemann[4] and later by Hudimoto[22]; it applies to cascades of zero-thickness parabolic airfoils with restrictions of small camber and small angle of attack. Actually the equation can also be obtained from the early results of Weinig[1] for circular arc cascades.

$$C_L = \frac{8 b_0 \sigma}{Q} \sin\alpha + \theta \frac{8\sigma^2}{\pi} \left[\tanh^{-1}(b_0^2)\right] \cos\alpha . \qquad (141)$$

For α of the order of θ this agrees with Equation (74) to order θ. Thus the results of early theory have been improved upon since the restriction of small angle of attack has been removed, resulting in the appearance of the term involving coefficient A_1 (see Equation (74)).

The cascade of zero-thickness S-shaped airfoils has been treated previously only by Klingemann for the case where the flow vector V_∞ is approximately parallel to a line tangent to the camber line at the midpoint. Klingemann obtained a series solution for the ratio $C_L/(C_L)_{\sigma=\infty}$; his series converges less rapidly as σ becomes smaller. If the present theory is applied to this special case, the result valid for σ large is

$$\frac{C_L}{(C_L)_{\sigma=\infty}} = 1 - \left(\frac{\pi}{\sigma}\right)^2 \frac{5}{64} \cos 2\beta + \theta\left(\frac{1}{\sigma^4}\right). \qquad (142)$$

Figure 7 shows the comparison for one value of stagger angle, of Equation (142) and the results of Klingemann. The good agreement in the range of σ where Equation (142) is accurate can be taken as a confirmation of the present theory. Again former restrictions on the angle of attack have been removed.

The theories used by Klingemann and Hudimoto to arrive at the results above, were mentioned in the Introduction, where it was pointed out that both incorporated conformal transformation. However the theory of Pistolesi[2] does not utilize conformal transformation. A comparison with his work is thus of independent interest. Pistolesi did not use the exact flat plate cascade solution as a basis, since it involves conformal transformation. Thus his solution for this simplified case is already an approximation. His result for lift coefficient of a flat plate cascade is

$$\frac{C_L}{(C_L)_{\sigma=\infty}} = \frac{2\frac{\sigma}{\pi}}{Re\left[e^{i(\alpha+\beta)}\coth\left(\frac{\pi}{2\sigma}e^{i(\alpha+\beta)}\right)\right]} \tag{143}$$

whereas the exact solution is

$$\frac{C_L}{(C_L)_{\sigma=\infty}} = \frac{4\frac{\sigma}{\pi}b_0}{\sqrt{1+b_0^4+2b_0^2\cos 2\beta}} \tag{144}$$

Pistolesi's equation is in terms of geometrical parameters only - that is, it does not involve b_0. This is a convenience provided Equation (143) is accurate. But Equation (143) implies a dependence upon α which is not shown by Equation (144). Thus Pistolesi's results are obviously incorrect. Computation shows Pistolesi's equation gives a value 8 $^{o}/o$ too high for the case $\sigma = 1$, $\beta = 45^{o}$, $\alpha = 0$.

Since Pistolesi's results for the flat plate are incorrect, it is quite unlikely that his treatment of the arbitrary airfoil is better. His equations are not in a form suitable for comparison by inspection - instead computations must be made. Thus no comparison with his more general case will be attempted here. Instead this discussion of the Pistolesi theory will be concluded with a discussion of the source of error.

The Birnbaum-Glauert theory for the single airfoil gives the following equation for C_L at small α for the flat plate airfoil:

$$C_L = 2\pi\alpha . \tag{145}$$

If terms of order α^2 and higher are neglected the exact theory gives the same equation. However it was shown above that no such agreement occurs for the extension to the cascade by Pistolesi. Part of the reason for this is the introduction of stagger angle and spacing, parameters not found in the case of the single airfoil. As Pistolesi pointed out, for a cascade the velocity induced at the chord line by the vortex distribution is not necessarily perpendicular to the chord line as in the case of a single airfoil. The component of induced velocity parallel to the chord line was neglected by Pistolesi. This is part of the reason for the discrepancy.

Another source of error can be seen in the Pistolesi theory. For the single airfoil, only the first two coefficients in Glauert's Fourier series contribute to the circulation - the rest can be neglected without introducing error. On the other hand Pistolesi showed that all coefficients affect the circulation in the case of the cascade. Yet he neglected all but the first two or three.

Thus there are at least two sources of error in the Pistolesi cascade theory which do not occur in single airfoil theory.

B. Deviation Angle

Weinig[1] lists a deviation angle formula for zero-thickness cascades with two restrictions:

(1) $\sigma < 0.7$

(2) curvature of the camber line at the trailing edge of the order of σ.

His formula is

$$\delta = (\text{curvature at the trailing edge}) \frac{\sigma}{\pi} A \cos\beta .$$

For the cubic camber line of this paper the formula reduces to

$$\delta = (\theta + 3\mu) \frac{\sigma}{\pi} A \cos\beta . \tag{147}$$

The same equation can be obtained from the present theory (Equations (78), (93) and (96)) if terms of order σ^2, ϵ, μ^2, θ^2, and higher are neglected. The equations of present theory are therefore a considerable extension of the previous analytical equation for deviation angle.

Shirakura[33] has used his exact numerical method to calculate flow characteristics for four zero-stagger, zero-thickness circular arc cascades. His results for deviation angle are compared in Table I with Equation (78). The agreement is excellent, despite the large camber angles.

In an actual cascade the assumptions of the present theory are invalid to various degrees - the flow is not strictly two-dimensional and does not satisfy the criteria of potential flow; the same is true in an actual turbomachine. A comparison of experimental results with those

Table I. Deviation Angle Comparison

Case	σ	θ	γ_u	Deviation Angle Shirakura	Deviation Angle Equation (78)
1a	0.5	$87^\circ\ 12'$	$-34^\circ\ 15'$	$9^\circ\ 21'$	$9^\circ\ 27'$
1b	"	"	$34^\circ\ 11'$	$9^\circ\ 25'$	$9^\circ\ 37'$
2a	0.7	"	$-31^\circ\ 19'$	$12^\circ\ 17'$	$12^\circ\ 32'$
2b	"	"	$30^\circ\ 52'$	$12^\circ\ 44'$	$13^\circ\ 19'$
3a	1.0	"	$-28^\circ\ 8'$	$15^\circ\ 28'$	$15^\circ\ 40'$
3b	"	"	$26^\circ\ 17'$	$17^\circ\ 19'$	$18^\circ\ 17'$
4a	0.5	$123^\circ\ 52'$	$-48^\circ\ 58'$	$12^\circ\ 58'$	$13^\circ\ 24'$
4b	"	"	0	13°	$13^\circ\ 32'$
4c	"	"	$48^\circ\ 55'$	$13^\circ\ 1'$	$13^\circ\ 40'$

of the present theory would be of considerable interest, but will not be attempted here because of its scope. However mention will be made of a comparison with a well-known empirical deviation angle formula based on experimental cascade data. This comparison was made before the portion of the theory dealing with thickness was contrived, hence the airfoils were assumed to be of zero thickness. It was found that for $0.8 < \sigma < 1.4$, Equation (78) gives values in fair agreement with the rule of Constant, devised for use under certain restricted conditions[9], but now used in the simple form[45]

$$\delta = 0.26\,\theta\sqrt{\sigma} \tag{148}$$

The discrepancies were of the order of magnitude of those between various empirical rules, such as Constant's rule and one used by Messrs. Power Jets (reference 46, Figure 26). It therefore appears that the combined influence of thickness, viscosity, compressibility, etc., on deviation angle may be small, at least in the experimental cascades which were used to devise the empirical rules. The work of Bowen, Sabersky, and Rannie[45] also tends to indicate this. A more extensive comparison with experiments is necessary for determination of the limits of this correlation, but it seems reasonable at the present state of knowledge of turbomachines to conclude that:

> If zero thickness is assumed the present first-order theory gives overall flow characteristics in fair agreement with experimental values for compressor cascades.

This is very fortunate because Equation (78) is easy to use, particularly if the approximate formulas (Equations (93) and (96)) are used for coefficients, whereas including the effect of thickness is a relatively lengthy procedure. For values of σ outside the range in which agreement with Constant's rule is obtained, Equation (78) undoubtedly gives better values than the empirical rule.

C. Smooth Entry

Weinig[1] has derived the following equations for smooth entry condition for a circular arc cascade:

$$\Omega = \theta\,\frac{4\sigma}{\pi}\cos\beta\,\tanh^{-1}\left(b_0^2\right) \tag{149}$$

$$\beta = \frac{\gamma_U + \gamma_D}{2} . \tag{150}$$

The first of these agrees with Equation (112) to order θ^3; the second agrees with Equation (114) to order θ^2.

The upstream flow angle for smooth entry was calculated by Shirakura[33] for the four cascades of Table I. Table II shows a comparison of his results with those obtained from the present theory. Again there is good agreement.

Table II. Smooth Entry Comparison

Case	θ	σ	γ_U for Smooth Entry	
			Shirakura	Present
1	$87^\circ\ 12'$	0.5	$34^\circ\ 11'$	$34^\circ\ 1'$
2	"	0.7	$30^\circ\ 52'$	$30^\circ\ 24'$
3	"	1.0	$26^\circ\ 17'$	$25^\circ\ 42'$
4	$123^\circ\ 52'$	0.5	$48^\circ\ 55'$	$48^\circ\ 20'$

D. Velocity and Pressure Distribution

Apparently there are no explicit analytical solutions in the literature for velocity or pressure distribution in an arbitrary cascade. A comparison must therefore be restricted to specific cases for which numerical methods have been used.

Two cases are available for zero-thickness airfoil cascades, both with circular arc airfoils: Weinig[1] has calculated the velocity distribution for smooth entry for the case $\sigma = 0.7$, $\beta = 45^\circ$, $\theta = 60^\circ$; Shirakura[33] has calculated pressure distribution for smooth entry for

case 4 of Tables I and II. Comparison of the present first order theory (Equations (116) and (119)) with the computations of Weinig is shown in Figure 8. The agreement is only fair due to the large camber angle. Since the camber angle of the Shirakura case is even greater, a comparison is not given here.

To test the portion of the present theory dealing with airfoil thickness, the ideal example for comparison is a cascade of airfoils having straight camber lines. No such example has been found in the literature. The next best alternatives are cascades with circular arc, parabolic, or cubic camber lines. Here again no reliable computation is available. Instead two examples have been selected: the first is not a cascade but does have a straight camber line, and the second is a cascade with a camber line which differs from the three types of this paper.

The first example is the NACA 0010 single airfoil at zero angle of attack. This case was calculated by Garrick[47] in 1933 and apparently done again (the results are slightly different) by Abbott, von Doenhoff, and Stivers[48] in 1945. In each case the results were listed by the authors in tabular form. Figure 9 shows a comparison with present theory; the agreement is excellent.

The second example chosen has a camber line composed of portions of two parabolas. Notching this camber line with a cubic is, of course, approximate and introduces additional errors into the solution. This example was originally calculated by Garrick[5] and has been verified by other methods by Katzoff et al[36] and Woolard[37]. The comparison is shown in Figure 10. The discrepancies can probably be assumed to be due to the difficulties in matching the camber line.

IV. DISCUSSION

In this section the solution is first examined for what it discloses about the flow. Next an attempt is made to evaluate the accuracy of the present first-order solution. Finally some aspects of the practical use of the results are discussed.

A. Insight Afforded by the Solution

The agreement with the analytical results of Weinig, Klingemann, and Hudimoto confirms to some extent the validity of the present results as formal power series expansions. Further confirmation awaits an exact solution, or approximations obtained in other ways. The solution will now be assumed to be correct and examined for the information it discloses.

The greater complexity of the cascade flow compared to that about a single airfoil is certainly well borne out by the results. The two additional parameters σ and β appear in the equations as well as the quantity b_0. Though b_0 is a function of σ and β it cannot be eliminated from the results without approximation because of the form of Equation (5). This is true even in the exact solution of the flat plate cascade, and is unfortunate because it makes it difficult to see easily from the equations the influence of spacing or stagger alone. In the approximate formulas for certain coefficients (such as Equation (93)) this difficulty is not present since the parameter b_0 does not appear. In the case of airfoils with thickness, the separate influences of spacing and stagger are even more obscure, since the present special technique of solving the BVP (see Appendix B) could not be used. It appears therefore that spacing and stagger are very closely related in the theory of cascades.

In one sense the solution has welcome simplicity. Various complicated equations for airfoil shape can all be put in the simple form of Equation (135), due to the linearizing assumptions and the fact that the differences in airfoil construction are of second order. Thus flow characteristics for different cascades are seen to be equivalent, to the order of approximation used here, if the cascades differ only in the method of construction discussed in the Introduction.

Deviation angle is frequently used in axial-flow compressor design and theory in preference to lift coefficient, because the former is relatively independent of upstream conditions. In the case of circular arc airfoils, Equations (79) and (80) show that in general δ is dependent upon γ_U, and Equations (97) and (98) show that for large σ (that is, for conditions approximating the single airfoil), it is influenced markedly by upstream conditions. However most axial flow compressor designs involve high enough solidities for σ to be in the range expressed by Equation (101). In this case Equations (93) and (96) indicate δ is relatively insensitive to γ_U. In fact if σ is less than about 0.7 (i.e., if solidity is greater than about 1.4) terms of order ϵ and higher can be neglected and the present theory gives

$$\delta = \theta \frac{\sigma}{\pi} A \cos\beta \tag{151}$$

which is completely independent of γ_U. This is easily explained physically: if spacing is sufficiently small, the exit flow direction is influenced primarily by the geometry of the airfoils near the trailing edge and conditions upstream are unimportant.

The present first-order results for smooth entry conditions are interesting. From Equations (112), (115), (130), and (131),

$$\Omega = \theta \Omega_1^{(\theta)} \tag{152}$$

$$\beta = \frac{\gamma_U + \gamma_D}{2} + \mu \beta_1^{(\mu)} \tag{153}$$

Thus turning angle is influenced only by the amount of camber and is independent of the amount of S-shape. Furthermore airfoil orientation is unaffected by camber angle, but is dependent upon S-angle. Thus if upstream and downstream conditions are given, the camber angle required for smooth entry is fixed, whereas the S-angle may be established by other considerations, such as pressure distribution. Final choice of S-angle then determines the actual airfoil orientation to assure smooth entry. It should be emphasized that these conclusions are based only on first-order results.

For the single airfoil with small angle of attack, the thickness does not enter into the first-order expression for circulation. However in the case of a cascade, Equations (57) and (60) indicate that thickness can have an effect on b and ψ and hence, theoretically, on circulation and other overall flow characteristics. The theory of Pistolesi[2] indicates the same conclusion. Actually the agreement between deviation angles predicted by the present theory for zero-thickness airfoil cascades with those predicted by empirical formulas for actual cascades suggests that the net effect of thickness plus all variables neglected in the present theory, is small. Thus for best practical results thickness should be ignored in the determination of overall flow characteristics. Of course this is not valid for velocity and pressure distribution, where

thickness plays an important role.

It is interesting to compare the present analysis with former theories on the basis of the model established to approximate the airfoil. In general the approximation used here consists of neglecting higher powers of the linearization parameters. Thus the transformation equation $w = w(z)$, without higher order terms, relates the unit circle and an airfoil with a shape which approximates the given shape. The approximate contour is a line which deviates from the given contour, probably crossing it in a number of places. This is obviously an entirely different model than a distribution of singularities on the chord line, as used in former theories.

The remainder of this discussion on the insight afforded by the solution will be devoted to the velocity distribution.

It is significant that the velocity distribution was left in terms of b and ψ (see Equation (139)), while other flow characteristics (such as δ) were reduced to simple series form by means of substitutions for b and ψ. The reason is that velocity distribution, considered as a function of θ, μ, τ, and ϕ, has certain non-linearities which make it impossible to write a uniformly convergent series of the type found for δ, except in the special case of smooth entry (see Equation (116)). These non-linearities in the velocity occur at the leading edge, and are not difficult to illustrate by examples.

As a simple example of a leading edge non-linearity, consider the case of a cascade of flat plate airfoils with upstream velocity vector parallel to the chord. The velocity is a constant everywhere in the flow field. Now if the airfoil shape is changed to a circular arc and the up-

stream flow direction is left unchanged, the velocity at the leading edge becomes infinite, regardless of how small the camber angle, provided it is not zero. Because of this singularity, velocity at the leading edge is certainly a non-linear function of camber angle.

Similarly the velocity at the leading edge is a non-linear function of thickness because if thickness is added to the flat plates in the previous case, this velocity becomes zero regardless of how small the maximum thickness, provided it is not zero. This is non-linearity in the form of a discontinuity, in contrast to the singularity above.

Non-linearities at the leading edge are also present in single airfoil theory, and are the primary reason for the frequent failure of early theories to correctly predict velocity. In the more recent and very elegant theory of Lighthill[17] a non-linear equation for velocity is given.

The present theory has a decided advantage over former theories in that leading edge difficulties do not arise. This is because the solution is derived from conformal transformation, and velocity is expressed as the absolute value of the ratio of $\frac{dP}{dz}$ to $\frac{dw}{dz}$. For the first case above (flat plates) the ratio for the velocity at the leading edge is the indeterminate form $0/0$, which can be shown by L'Hospital's rule to have the proper limiting value. The change to a circular arc changes the numerator to a small but finite number, giving the required singularity in velocity. Similarly the change to finite thickness changes the denominator, giving the proper discontinuity. Thus the present theory, though based on linearization, is capable of correctly describing these distinctly non-linear relationships.

It can be seen from Equation (139) that variations of the slope of

the airfoil contour influence the velocity distribution, since the derivatives u_1', v_1', etc., occur in the denominator. This is also shown by the equations of Garrick[5], although somewhat less clearly. Thus an airfoil contour may be continuous, but if the slope is discontinuous, there will (theoretically) be discontinuities in velocity distribution. Apparently the curvature may be discontinuous without producing a velocity discontinuity, but a sudden change will occur in the velocity gradient along the airfoil surface. The latter effect is known to influence boundary layer performance.

It was stated in the Introduction that velocity and pressure distribution were more difficult to determine accurately than overall flow characteristics. This was evident in the previous section, where the results of Shirakura were very closely matched for deviation angle (Table I) but poorly matched for pressure distribution. The reason for this is quite simple: the overall flow characteristics are not as sensitive to airfoil contour as are velocity and pressure distribution. This is quite obvious since the lift is essentially an average of the pressure distribution.

B. Accuracy of the Present First-Order Solution

The approximate theories of Klingemann[4] and Hudimoto[22] were based on the assumption that the cascade airfoils deviate little from straight lines, but no indication was given by these authors of the amount of error involved in this assumption. The present theory is based on the same premise and the first-order approximation gives the same results for overall flow characteristics, aside from a removal of restrictions on angle of attack. However the present theory differs from

the earlier theories in several important respects, not the least of which is its usefulness for finding higher order approximations. These are useful for evaluation of the accuracy of the first-order solution. By way of example, the deviation angle will be considered in the following.

It is believed that the higher order terms due to camber are the most important, and that those due to thickness and S-shape need not be considered for axial flow compressors. As pointed out in Part II the higher order terms are relatively difficult to obtain and interpret. However a simplified expression, valid only for high solidity, (Equation (104)) was obtained for the second-order coefficient $\delta_2^{(\theta)}$ in the equation for deviation angle of a circular arc cascade (Equation (103)). A plot of the ratio $\delta_2^{(\theta)} / \delta_1^{(\theta)}$ computed from this equation is shown in Figure 5. The limitations of this figure are discussed in the Analysis and should be kept in mind. For constant β, the absolute value of the ratio is seen to be highest at $\sigma = 0$ (zero spacing or infinite solidity), decreasing with increasing σ. The plot is discontinued at values of σ somewhat less than 1.0, since the equation for $\delta_2^{(\theta)} / \delta_1^{(\theta)}$ is invalid for large σ. The exact equation for deviation angle at $\sigma = \infty$ (single airfoil) is known, namely

$$\delta = \alpha + \frac{\theta}{2} \qquad \text{for} \qquad \sigma = \infty . \tag{154}$$

Here obviously $\delta_2^{(\theta)} / \delta_1^{(\theta)} = 0$, indicating that the curves of Figure 5 approach the value zero as σ increases. Thus from Figure 5 one can state that:

(1) Except for β large, $\delta_2^{(\theta)}$ is less in absolute value than $\delta_1^{(\theta)}$.

(2) If β is positive, $\delta_2^{(\theta)}$ and $\delta_1^{(\theta)}$ are of opposite sign.

(3) The ratio $\delta_2^{(\theta)} / \delta_1^{(\theta)}$ decreases in absolute value with σ.

(4) For fixed β, the ratio $\delta_2^{(\theta)}/\delta_1^{(\theta)}$ is about half as large at $\sigma = 0.5$ as at $\sigma = 0$.

The following assumptions enable an error analysis to be made:

(I) The errors due to thickness and S-shape can be neglected.

(II) The error in δ resulting from the use of first-order terms alone is less in absolute value than $\left| \theta^2 \delta_2^{(\theta)} \right|$.

(III) The value of σ is greater than 0.5 (solidity < 2.0).

The first assumption follows from a statement above about the importance of higher order terms due to camber. The second follows from the first two statements made regarding Figure 5 and the indication that the coefficients alternate in sign. The third assumption follows from present axial flow compressor practice.

Under these assumptions an approximate equation for the maximum error can be written:

$$\frac{\text{maximum error in } \delta}{\delta} = \left| \frac{\theta}{2} \left(\delta_2^{(\theta)} / \delta_1^{(\theta)} \right)_{\sigma=0} \right| . \tag{155}$$

Substitutions from Equations (104) and (105) lead to

$$\frac{\text{maximum error in } \delta}{\delta} = \left| \frac{\theta}{4} \left[\frac{\beta}{(\log_2 \cos\beta + \beta \tan\beta)\cos^2\beta} - \tan\beta \right] \right| . \tag{156}$$

Thus a relatively simple expression has been obtained for the maximum error introduced by using the present first-order equation for deviation angle. Refinements of this formula are possible, of course, but will not be attempted here.

Equation (156) implies that error increases with β. This is reasonable since the distance between airfoils decreases with β, if σ

remains constant. (See Figure 3). Equation (156) also implies that error is zero if $\beta = 0$. The comparison with the numerical results of Shirakura in Table I indicates the error is, of course, not zero when $\beta = 0$, but is very small, not exceeding one percent of the camber angle. The maximum stagger angle β encountered in axial flow compressors is about 70°. If the maximum error in deviation angle must be less than, say, five percent of the deviation angle, the camber angle should not exceed about 15° as can be shown using Equation (156). For $\beta = 30^{\circ}$ the camber angle can be as large as 45° without the error exceeding five percent of δ. For cases where Equation (156) indicates more error than is allowable, higher order terms cannot be neglected.

The foregoing error analysis was concerned with the deviation angle equation. It might be supposed that the same conclusions would be reached from a similar analysis for other flow characteristics. Actually this does not occur; the linearized equations for C_L, Γ, and $\tan\gamma_D$ are <u>not</u> as accurate as the equation for δ. (Since $\Omega = \gamma_U - \delta + \beta - \gamma_T$, the linearized equation for turning angle has the same error, as the δ equation). This apparent paradox can be explained by the fact that δ and Ω are apparently very nearly linear functions of θ, while the other overall flow characteristics are not. This is shown clearly for a particular case by the curves of Figure 11 which were constructed not from the results of the present theory, but from the numerical results of Shirakura in Table I. The curve for δ is much more nearly linear than that for C_L. Hence the linearized formula for δ is more accurate than that for C_L. The physical reason for this situation is not entirely clear. However for maximum numerical accuracy, the deviation angle

should be computed from an equation such as Equation (78), and if C_L is required, this number should be used to compute C_L, rather than a direct linearized formula, such as Equation (74).

No error analysis has been attempted with regard to the present results for velocity distribution. However the range of permissible camber ange (for a given error) is probably less than in the case of deviation angle, as indicated by the example in Figure 8.

C. Practical Use of the Results

Axial flow compressors are usually designed for efficient and stable operation at a given set of conditions, normally called the "design point". Potential flow is frequently assumed first, necessary corrections being applied at subsequent points in the design procedure. An initial three-dimensional treatment of the problem has the object of fixing the conditions ahead and behind each row of blades. When the number of blades in each row is fixed, each circumferential section of blading can be regarded as a two-dimensional cascade in which upstream and downstream conditions are specified, and the cascade geometry must be determined. This is an example of the inverse cascade problem mentioned in the Introduction.

This design point cascade problem is readily solved using the results of the present theory. In Part III it was shown that overall flow characteristics of an actual compressor cascade can apparently be approximated sufficiently well by assuming the airfoils have zero-thickness and using the present equations. Thus only the shape of the camber line and its orientation in the cascade must be determined. The use of smooth entry as design condition is particularly convenient, and results in the following procedure:

Using Equation (153), a first approximation for β can be written

$$\beta = \frac{\gamma_U + \gamma_D}{2} \quad (157)$$

The airfoil spacing is known, hence σ can now be easily found. With the values of σ and β, camber angle can be found from Equation (152) in the form

$$\theta = \frac{\pi}{4\sigma} \frac{\gamma_U - \gamma_D}{\cos\beta \tanh^{-1}(b_0^2)} . \quad (158)$$

It is convenient to plot the reciprocal of the coefficient of $\gamma_U - \gamma_D$ in Equation (158) as a function of σ and β, thus avoiding the computation each time of b_0 from Equation (5). Weinig has constructed such a graph (Reference 1, Figure 81). If no S-shape is to be included in the camber line, this completes the procedure. If a non-zero value of S-shape angle μ is selected, the camber angle is unchanged, but a second approximation to the stagger angle must be found. For axial flow compressors where the conditions

$$\epsilon = e^{2\beta\tan\beta - \frac{\pi}{\sigma\cos\beta}} < 0.4 , \quad \sigma < 1.25$$

are usually fulfilled, Equation (131) can be used in the form

$$\beta = \frac{\gamma_U + \gamma_D}{2} + \mu \left\{ \frac{1}{2} - \frac{3\sigma}{\pi} A\cos\beta + \frac{3\sigma^2}{\pi^2}\left(\frac{\pi^2}{12} + A^2\cos^2\beta\right) \right.$$

$$\left. - \epsilon \left[\frac{3\sigma}{\pi} A\cos\beta + \frac{6\sigma^2}{\pi^2}\left(\cos^2\beta - A\cos^2\beta - 2\sin^2\beta \log 2\cos\beta\right)\right] \right\} \quad (159)$$

where from Equation (94),

$$A = \log 2\cos\beta + \beta\tan\beta. \tag{160}$$

Here again the coefficient of μ should be plotted for convenience.

When the design point of the compressor has been treated, off-design conditions are usually studied. The present solution of the direct cascade problem is convenient to use for off-design conditions, but it is important to note that the assumptions of the present theory may be invalid if, for example, flow separation occurs. Thus good judgment is required in determining how far from design conditions the results may be used.

With cascade geometry fixed (as when studying off-design characteristics) the overall effect of the cascade is best expressed as deviation angle, using the equation

$$\delta = \delta_0 + \theta\,\delta_1^{(\theta)} + \mu\,\delta_1^{(\mu)} \tag{161}$$

where from Equations (93), (96), and (129)

$$\delta_0 = \epsilon\cos^2\beta\,(\tan\gamma_U - \tan\beta) \tag{162}$$

$$\delta_1^{(\theta)} = \frac{\sigma}{\pi}A\cos\beta - \epsilon\left(\frac{1}{2} + \frac{\sigma}{\pi}\cos\beta - \frac{\sigma}{\pi}A\cos\beta\right) \tag{163}$$

$$\begin{aligned}\delta_1^{(\mu)} = {} & \frac{3\sigma}{\pi}A\cos\beta - \frac{3\sigma^2}{\pi^2}\left(\frac{\pi^2}{12} + A^2\cos^2\beta\right) \\ & + \epsilon\left\{\frac{1}{2} + \frac{3\sigma}{\pi}\cos\beta - \frac{3\sigma}{\pi}A\cos\beta + \frac{6\sigma^2}{\pi^2}\left[\frac{1}{2}\left(\frac{\pi^2}{12} + A^2\cos^2\beta\right)\right.\right. \\ & \left. -2\log 2\cos\beta + (1 + \log 2\cos\beta - \beta\tan\beta)\cos^2\beta\right] \\ & - (\tan\gamma_U - \tan\beta)\left[\beta - 3\tan\beta\log 2\cos\beta + \frac{6\sigma}{\pi}(A^2 - \beta^2)\sin\beta\right. \\ & \left.\left. + \frac{4\sigma^2}{\pi^2}\left(\frac{\beta^3}{\cos^3\beta} - A^3\tan\beta\cos^2\beta\right)\right]\right\}.\end{aligned} \tag{164}$$

Again here graphical representations are very convenient.

Presumably the foregoing formulas are applicable to some extent to axial flow turbines, but no evaluation has been made in this regard.

For axial flow turbomachinery with blading having solidities generally less than 0.8 ($\sigma > 1.25$), such as fans, the approximations based on small σ are not sufficiently accurate, and the formulas involving b_0 , such as Equation (79), should be used instead.

For more detailed studies of the performance of an axial-flow turbomachine either at design or off-design conditions, velocity (or pressure) distribution is frequently required. The computations are more complex than those just described and will not be given in detail here. The velocity distribution can be computed from Equation (139), taking into account the airfoil thickness, which was deliberately neglected above. The pressure distribution can be found using Equation (21).

For mixed flow turbomachines and other instances where stream surfaces are not even approximately cylindrical, it is doubtful that the present results are useful except qualitatively.

For cases where the value of b_0 is frequently required, a plot of b_0 versus σ for various β is convenient and can be computed from Equation (5). Rannie gives a plot of $\log(1/b_o)$, which he obtained in this way (Reference 45, Figure 82), and other similar curves can be found[1], [5].

When flow characteristics are required for a given cascade which has a camber line differing from any of the cases considered here, a nearly equivalent cubic camber line can be used. There are numerous ways such a camber line can be chosen, and probably the differences are of minor importance. However one method - matching tangents at leading and trailing edges - is obviously not feasible with

NACA 65 series camber lines because these have infinite slopes at the leading and trailing edges. Instead an equivalent circular arc may be defined as having, say, the same maximum distance from the chord line.

The inverse hyperbolic tangent function occurs at several points in the present solution to the cascade problem. (See Equations (76) and (140) for example). Though it is not difficult to locate tables for real arguments, the function is also needed for complex arguments. The most readily available table is by Jahnke and Emde (Reference (49), Addenda, p. 72) but a much more extensive table occurs in a book by Hawelka (Reference 50, p. 55). Use can also be made of the following relation:

$$\tanh^{-1} z = \frac{1}{2} \log \frac{1+z}{1-z} . \tag{165}$$

To account for airfoil thickness a "conjugation" must be performed. Though one conjugation (to determine $u_1^{(\tau)}$ as a function of ϕ) suffices for any set of values of thickness, camber angle, and S-shape angle, a change in stagger angle or spacing requires a new conjugation. Curves or tables can be devised for each airfoil shape equation giving $u_1^{(\tau)}$ in terms of the three parameters ϕ, σ , and β .

If more than one airfoil shape equation is used, the number of curves or tables required can be diminished in some cases. For example the family of airfoil shape equations expressed by

$$y(x) = \pm \sum_{n=1}^{m} A_n \left(x+\tfrac{1}{2}\right)^{\frac{n}{2}} \tag{166}$$

can be reduced to no more than m-1 cases, which can be used for all

sets of the A_n. From Equation (166), $y(-\frac{1}{2}) = 0$ and since $y(\frac{1}{2}) = 0$ also, it follows that

$$\sum_{n=1}^{m} A_n = 0 . \tag{167}$$

Thus one can write

$$y(x) = \pm \sum_{n=1}^{m} A_n \left[(x+\tfrac{1}{2})^{\frac{n}{2}} - (x+\tfrac{1}{2}) \right] . \tag{168}$$

Then one may individually solve the set of m-1 BVP's whose equations, which are <u>independent</u> of the A_n, are

$$v_{1,n}^{(\tau)} = \pm \left[(2u_0+\tfrac{1}{2})^{\frac{n}{2}} - (2u_0+\tfrac{1}{2}) \right] \tag{169}$$

and add the solutions using

$$v_1^{(\tau)} = \sum_{n=1}^{m} A_n \, v_{1,n}^{(\tau)} . \tag{170}$$

The NACA four digit airfoil series has a thickness distribution similar to Equation (166), if some arbitrary rounding of the trailing edge is assumed. Other schemes can be devised for other thickness families.

The number of "points" (values of ϕ) used in a numerical method of conjugation influences the accuracy of the solution. Eighty points were used in the two examples with thickness given here, the conjugations being performed on a punch-card calculator.

To calculate velocity distribution on airfoils with thickness the derivative $u_1^{(\tau)'} = \frac{d u_1^{(\tau)}}{d\phi}$ is required. This can be obtained from the solution for $u_1^{(\tau)}$, but an alternative direct procedure is also possible. The function $izF_1^{(\tau)'}(z) = iz \frac{d}{dz} F_1^{(\tau)}(z)$ is regular in the same region as $F_1^{(\tau)}(z)$. If $|z| = 1$,

$$iz F_1^{(\tau)'} = u_1^{(\tau)'} + i v_1^{(\tau)'} . \tag{171}$$

Since $v_1^{(\tau)}$ is known, $v_1^{(\tau)\prime}$ is known. Hence $u_1^{(\tau)\prime}$ can be found by conjugation of $v_1^{(\tau)\prime}$. If both $u_1^{(\tau)}$ and $u_1^{(\tau)\prime}$ are needed, but only one conjugation is desirable, perhaps the one for $u_1^{(\tau)\prime}$ is the better one to perform, because $u_1^{(\tau)}$ can be found by integration, a more accurate numerical process than differentiation. The function $u_1^{(\tau)}$ found in this way must, of course, satisfy the BVP conditions.

REFERENCES

1. Weinig, F., "Die Strömung um die Schaufeln von Turbomaschinen", Leipzig: Barth, (1935).

2. Pistolesi, E., "On the Calculation of Flow Past an Infinite Screen of Thin Airfoils", NACA TM 968, (1941).

3. Glauert, H., "Aerofoil and Airscrew Theory", Cambridge, (1925).

4. Klingemann, G., "Verfahren zur Berechnung der Theoretischen Kennlinien von Turbomaschinen", Ingenieur-Archiv., 11, p. 151, (1940).

5. Garrick, I. E., "On the Potential Flow Past a Lattice of Arbitrary Airfoils", NACA Report 788, (1944).

6. Theodorsen, T., "Theory of Wing Sections of Arbitrary Shape", NACA Report 411, (1931).

7. Goldstein, S., "Approximate Two-Dimensional Aerofoil Theory", Parts I-VI, A.R.C. Technical Report C.P. 68-73, (1952).

8. Abbott, I., and von Doenhoff, A., "Theory of Wing Sections", New York: McGraw-Hill, (1949).

9. Howell, A. R., "The Present Basis of Axial Flow Compressor Design", Part I, R. and M. 2095, (1942).

10. Churchill, R., "Introduction to Complex Variables and Applications", New York: McGraw-Hill, (1948).

11. Theodorsen, T., and Garrick, I. E., "General Potential Theory of Arbitrary Wing Sections", NACA Report No. 452, (1933).

12. Milne-Thomson, L. M., "Theoretical Hydrodynamics", 2nd Ed., New York: Macmillan, (1950).

13. Pope, A., "Basic Wing and Airfoil Theory", New York: McGraw-Hill, (1951).

14. Durand, W. F., "Aerodynamic Theory", Vol. II, Pasadena: Durand Reprinting Committee, (1943).

15. Birnbaum, W., "Die tragende Wirbelfläche als Hilfsmittel zur Behandlung des ebenen Problems der Tragflügel Theorie", ZAMM 3, p. 290, (1923).

16. Jones, R. T., "Leading-Edge Singularities in Thin-Airfoil Theory", J. Aero. Sci. 17, p. 307, (1950).

17. Lighthill, M., "A New Approach to Thin Aerofoil Theory", Aero. Quarterly, 3, p. 193 (1951).

18. Munk, M., "General Theory of Thin Wing Sections", NACA TR 142, (1922).

19. Goldstein, S., "Low-Drag and Suction Airfoils", J. Aero. Sci. 15, p. 189, (1948).

20. Scholz, N., "On an Extension of Glauert's Theory of Thin Airfoils to Profiles in Cascade", J. Aero. Sci. 18, p. 637, (1951).

21. Lieblein, V., "The Calculation of the Lift Characteristics of an Aerofoil Section in a Cascade", British Reports and Translations No. 442, (1947).

22. Hudimoto, B., Kamimoto, G., and Hirose, K., "Theory of Wing Lattice", Engineering Research Institute, Kyoto University, Kyoto, Japan, 1, p. 71, (1951).

23. Naimen, I., "Numerical Evaluation by Harmonic Analysis of the ϵ - Function of the Theodorsen Arbitrary-Airfoil Potential Theory", NACA WR L153, (1945).

24. Watson, E. J., "Formulae for the Computation of the Functions Employed for Calculating the Velocity Distribution about a Given Aerofoil", R and M 2176, (1945).

25. Howell, A. R., "Note on the Theory of Arbitrary Aerofoils in Cascade", R.A.E. Note E3859, (1941).

26. Traupel, W., "Calculation of Potential Flow Through Blade Grids", Sulzer Technical Review, No. 1, p. 25, (1945).

27. Abe, S., "Theory for Characteristics of Straight Lattice Composed of Aero- or Hydro-foil Profiles of Arbitrary Form, Technology Reports of the Tohoku University, Sendai, Japan, 15, No. 2, (1951).

28. Merchant, W. and Collar, A. R., "Flow of an Ideal Fluid Past a Cascade of Blades", Part II, R and M 1893, (1941).

29. Lighthill, M. J., "A Mathematical Method of Cascade Design", R and M 2104, (1945).

30. Hirose, K., "On the Mapping of Cascades of Arbitrary Aerofoils", Trans. Japan Soc. Mech. Engr., 14, p. 111, (1948).

31. Moriya, T., "The Theory of Lattice Composed of Aerofoils of Arbitrary Profile Form", J. of Soc. Appl. Mech., Japan, 1, p. 576, (1941).

32. Mutterperl, Wm., "A Solution of the Direct and Inverse Potential Problems for Arbitrary Cascades of Airfoils", NACA WR L81, (1944).

33. Shirakura, M., "A Theory on Cascades Built up of Arbitrary Blade Sections", Japan Science Review, 2, p. 243, (1952).

34. Betz, A., "Diagrams for Calculation of Airfoil Lattices", NACA TM 1022, (1942).

35. Weinel, E., "Beiträge zur rationellen Hydrodynamik der Gitterströmung", Ing.-Arc., 5, p. 91, (1934).

36. Katzoff, S., Finn, R., and Laurence J., "Interference Method for Obtaining the Potential Flow Past an Arbitrary Cascade of Airfoils", NACA TN 1252, (1947).

37. Woolard, H., "The Incompressible Flow About a Cascade of Airfoils", Cornell Aero. Lab. Report AF-734-A-1, (1950).

38. Hutton, S., "Thin Aerofoil Theory and the Application of Analogous Methods to the Design of Kaplan Turbine Blades", Proc. Inst. Mech. Eng., England, 163, p. 81, (1950).

39. Stodola, A., "Steam and Gas Turbines", Vol. II, New York: Peter Smith, (1945).

40. Huppert, M., and MacGregor, C., "Comparison Between Predicted and Observed Performance of Gas-Turbine Stator Blade Designed for Free-Vortex Flow", NACA TN 1810, (1949).

41. Erdélyi, A., Magnus, W., Oberhettinger, F., and Tricomi, F., "Higher Transcendental Functions", New York: McGraw-Hill, (1953).

42. Nielsen, N., "Der Eulersch Dilogarithmus und seine Verallgemeinerungen", Abh. der Kaiserl Leop.-Carol. Deutschen Akad. der Naturforscher, 90, p. 125, (1909).

43. Spence, W., "An Essay on the Theory of the Various Orders of Logarithmic Transcendents", Mathematical Essays, London and Edinburgh, England, (1820).

44. Fletcher, A., Miller, J., and Rosenhead, L., "An Index of Mathematical Tables", New York: McGraw-Hill, (1946).

45. Bowen, J. T., Sabersky, R. H., and Rannie, W. D., "Theoretical and Experimental Investigations of Axial Flow Compressors", Report on Research conducted under Contract with the Office of Naval Research, California Institute of Technology, Pasadena, (1949).

46. Carter, A. D. S., and Hughes, Hazel P., "A Theoretical Investigation into the Effect of Profile Shape on the Performance of Aerofoils in Cascade", R. and M. 2384, (1950).

47. Garrick, I. E., "Determination of the Theoretical Pressure Distribution for Twenty Airfoils", NACA TR 465, (1933).

48. Abbott, I. H., von Doenhoff, A. E., and Stivers, L. S., Jr., "Summary of Airfoil Data", NACA TR 824, (1945).

49. Jahnke, E., and Emde, F., "Tables of Functions with Formulae and Curves", Fourth Edition, New York: Dover Publications, (1945).

50. Hawelka, R., "Vierstellige Tafeln der Kreis-und Hyperbelfunktionen, sowie ihrer Umkehrfunktionen im Komplexen," Berlin: Elektrotechnischer Verein (Printed Braunschweig: Vieweg, (1931).

APPENDIX A - NOTATION

a_{2n+1}	Laurent coefficient (see Appendix B)
A	$\log 2 \cos \beta + \beta \tan \beta$
A_0, A_1	Coefficients in equation for C_L
A_n	Complex coefficients in Theodorsen method
A_n	Real coefficient in conjugation discussion
b	Parameter locating singularities near circle
b_0, b_1, $b_1^{(\mu)}$, $b_1^{(\tau)}$	Coefficients in equation for b
B_1	Coefficient in equation for C_L
B_n	Complex coefficients in Rannie method
C	Coefficient in the equation for $\tan \gamma_D$
C_0, C_1	Coefficients in the equation for C
C_L	Lift coefficient
d_{2n}	Laurent coefficient (see Appendix B)
D	Coefficient in the equation for $\tan \gamma_D$
D_0, D_1	Coefficients in the equation for D
f(x)	Thickness function
F(z)	$\frac{\sigma}{\pi} e^{i\beta} \tanh^{-1}(b/z)$
$F_0(z)$	$\frac{\sigma}{\pi} e^{i\beta} \tanh^{-1}(b_0/z)$
$F_1(z)$	Function in equation for w(z)
$F_1^{(\phi)}(z)$, $F_1^{(\mu)}(z)$, $F_1^{(\tau)}(z)$	Solutions of auxiliary boundary value problems
$g_n(x)$	Airfoil shape functions
ℓ	Point on circle corresponding to leading edge
L	Leading edge of airfoil
n	Index
P	Static pressure

P_∞	Static pressure corresponding to V_∞
$P(z)$	Complex velocity potential
Q	$\sqrt{1+b_0^4+2b_0^2\cos 2\beta}$
r	Modulus of z
t	Point on circle corresponding to trailing edge
T	Trailing edge of airfoil
$u_0(r,\phi)$, $u_1(r,\phi)$, etc.	Real parts of $F_0(z)$, $F_1(z)$, etc.
$v_0(r,\phi)$, $v_1(r,\phi)$, etc.	Imaginary part of $F_0(z)$, $F_1(z)$, etc.
V	Flow velocity on airfoils
V_D	Flow velocity far downstream of cascade
V_U	Flow velocity far upstream of cascade
V_{vortex}	Velocity due to vortex distribution
V_∞	Vector average of V_U and V_D
$w = x + iy$	Complex variable in physical (cascade) plane
$w = w(z)$	Transformation equation
$x(r,\phi)$	Real part of w(z)
$y(r,\phi)$	Imaginary part of w(z)
$y(x,\eta)$	Airfoil shape function
$z = re^{i\phi}$	Complex variable in circle plane
α	Angle of attack
β	Stagger angle
$\beta_0, \beta_1^{(\mu)}$	Coefficients in equation for stagger angle
$\gamma = \alpha + \beta$	Angle giving direction of V_∞
γ_U, γ_D	Flow direction angles far up- and downstream
Γ	Circulation about one airfoil

δ	Deviation angle
$\delta_0,\ \delta_1^{(\theta)},\ \delta_2^{(\theta)},\ \delta_1^{(\mu)}$	Coefficients in equations for δ
Δ	Real quantity used in Rannie's method
Δ	Linearization parameter
ϵ	$e^{2\beta \tan\beta - \frac{\pi}{\sigma\cos\beta}}$
ζ	Complex variable
η	Linearization parameter
θ	Camber angle
λ	Point on circle corresponding to leading edge
μ	S-shape angle
ν_L, ν_T	Geometrical angles (see Figure 6)
ξ	Integration variable
ρ	Fluid density
σ	Spacing-chord ratio (note solidity = $1/\sigma$)
τ	Point on circle corresponding to trailing edge
τ	Maximum thickness-chord ratio
ϕ	Argument of z
ψ	Trailing edge argument
$\psi_0, \psi_1^{(\theta)}, \psi_1^{(\mu)}, \psi_1^{(\tau)}$	Coefficients in equations for ψ
$\Omega = \gamma_U - \gamma_D$	Flow turning angle
$\Omega_1^{(\theta)}$	Coefficient in equation for Ω
$(\ )_t,\ (\ )_\tau,\ (\ )_\ell,\ (\ )_\lambda$	Evaluation at points t, τ, ℓ, and λ
$(\ )_{\sigma=\infty}$	Single airfoil case
$(\ )_{\sigma=0}$	Infinite solidity case
$\frac{d}{dz}$	Complex derivative with respect to z
$\frac{\partial}{\partial\phi}$	Partial derivative with respect to ϕ

$( )'$	$\frac{d}{dz}$ or $\frac{\partial}{\partial \varphi}$
$( )'$	Rotated cascade (see smooth entry)
$\overline{( )}$	Complex conjugate
$\mathcal{I}m$	Imaginary part of
$\mathcal{R}e$	Real part of
$\mathcal{O}( )$	Terms of the order of
$\| \|$	Modulus of
$<$	Less than

APPENDIX B

DERIVATION OF THE FUNCTION $F_1^{(\theta)}(z)$

The function $F_1^{(\theta)}(z) = u_1^{(\theta)}(r,\phi) + iv_1^{(\theta)}(r,\phi)$, as used in the text is defined by three conditions:

(1) $F_1^{(\theta)}(z)$ is regular everywhere in the region $|z| \geq 1$.

(2) $v_1^{(\theta)}(1,\phi) = \frac{1}{8} - 2\left[u_0(1,\phi)\right]^2$, where $u_0(r,\phi)$ is known.

(3) $u_1^{(\theta)}(1,\psi_0) + u_1^{(\theta)}(1,\pi+\psi_0) = 0$.

These conditions indicate that $F_1^{(\theta)}(z)$ is the solution of a familiar type of potential theory problem: Find a function regular without and on a boundary, given its imaginary part on the boundary. The problem may be solved by using one of the Poisson formulas. In this case, however, a method is adopted which utilizes Laurent expansion coefficients.

The known function $F_0(z)$ follows, along with its Laurent expansion, valid in $|z| \geq 1$:

$$F_0(z) = \frac{\sigma}{\pi} e^{i\beta} \tanh^{-1}\left(\frac{b_0}{z}\right) = \frac{\sigma}{\pi} e^{i\beta} \sum_{n=0}^{\infty} \frac{(b_0/z)^{2n+1}}{2n+1} \tag{B1}$$

For convenience, the following form will be used for the expansion:

$$F_0(z) = \sum_{n=0}^{\infty} \frac{a_{2n+1}}{z^{2n+1}} \tag{B2}$$

where

$$a_{2n+1} = \frac{\sigma}{\pi b_0^{2n+1}} e^{i\beta} \int_0^{b_0^2} \xi^{2n}\, d\xi \,. \tag{B3}$$

From Equation (B2) and the definition of a conjugate complex function

$$\overline{F_0}\left(\frac{1}{z}\right) = \sum_{n=0}^{\infty} \overline{a}_{2n+1}\, z^{2n+1} \,. \tag{B4}$$

If one defines $a_{-(2n+1)}$ by the equation

$$a_{-(2n+1)} = \bar{a}_{2n+1} = \frac{\sigma}{\pi b_o^{2n+1}} e^{-i\beta} \int_0^{b_o^2} \xi^{2n} d\xi \tag{B5}$$

then from Equation (B4),

$$\bar{F}_o\left(\frac{1}{z}\right) = \sum_{n=0}^{\infty} a_{-(2n+1)} z^{2n+1} . \tag{B6}$$

Now $u_0(1,\phi)$ can be expressed in the form

$$u_o(1,\phi) = \frac{1}{2}\left[F_o(e^{i\phi}) + \bar{F}_o(e^{-i\phi})\right] . \tag{B7}$$

Using a similar expression for $v_1^{(\theta)}(1,\phi)$ condition (2) may be written

$$i F_1^{(\theta)}(e^{i\phi}) - i \bar{F}_1^{(\theta)}(e^{-i\phi}) = -\frac{1}{4} + \left[F_o(e^{i\phi})\right]^2 + \left[\bar{F}_o(e^{-i\phi})\right]^2 + 2 F_o(e^{i\phi}) \bar{F}_o(e^{-i\phi}) . \tag{B8}$$

The product in the last term in Equation (B8) may be expressed as the expansion

$$F_o(e^{i\phi}) \bar{F}_o(e^{-i\phi}) = \sum_{n=0}^{\infty} d_{2n} e^{-i2n\phi} + \sum_{n=1}^{\infty} d_{-2n} e^{i2n\phi} \tag{B9}$$

where

$$d_{2n} = \sum_{t=0}^{\infty} a_{-(2t+1)} a_{2n+2t+1} \tag{B10}$$

$$d_{-2n} = \sum_{t=0}^{\infty} a_{2t+1} a_{-(2n+2t+1)} . \tag{B11}$$

Substituting Equation (B9) into Equation (B8) results in

$$\begin{aligned} i F_1^{(\theta)}(e^{i\phi}) - i \bar{F}_1^{(\theta)}(e^{-i\phi}) = {} & -\frac{1}{8} + \left[F_o(e^{i\phi})\right]^2 + d_o + 2 \sum_{n=1}^{\infty} d_{2n} e^{-i2n\phi} \\ & -\frac{1}{8} + \left[\bar{F}_o(e^{-i\phi})\right]^2 + d_o + 2 \sum_{n=1}^{\infty} d_{-2n} e^{i2n\phi} \end{aligned} \tag{B12}$$

Thus by inspection

$$i F_1^{(\theta)}(e^{i\phi}) = -\frac{1}{8} + \left[F_0(e^{i\phi})\right]^2 + d_0 + 2\sum_{n=1}^{\infty} d_{2n} e^{-i2n\phi} + i\,(\text{constant}). \quad \text{(B13)}$$

Therefore

$$F_1^{(\theta)}(z) = \frac{i}{8} - i\left[F_0(z)\right]^2 - i d_0 - i 2\sum_{n=1}^{\infty} \frac{d_{2n}}{z^{2n}} + \text{constant}. \quad \text{(B14)}$$

Conditions (1) and (2) define $F_1^{(\theta)}(z)$ to within a real constant, which is fixed by condition (3). By inspection of Equation (B2), $F_0(e^{i\psi_0}) = -F_0(e^{i(\pi+\psi_0)})$, hence from Equation (B14), $F_1^{(\theta)}(e^{i\psi_0}) = F_1^{(\theta)}(e^{i(\pi+\psi_0)})$, and

$$u_1^{(\theta)}(1, \psi_0) - u_1^{(\theta)}(1, \pi + \psi_0) = 0. \quad \text{(B15)}$$

From this equation and condition (3), the constant in Equation (B14) can be evaluated, so that Equation (B14) becomes

$$F_1^{(\theta)}(z) = \frac{i}{8} - i\left[F_0(z)\right]^2 - i d_0 - i 2\sum_{n=1}^{\infty} \frac{d_{2n}}{z^{2n}} - 2u_0(1, \psi_0)\, v_0(1, \psi_0) - 2\,\mathrm{Im}\sum_{n=1}^{\infty} d_{2n} e^{-i2n\psi_0}. \quad \text{(B16)}$$

To put $F_1^{(\theta)}(z)$ in final form the terms in Equation (B16) involving coefficient d_{2n} are modified. From Equations (B3), (B5), and (B11),

$$d_0 = \sum_{t=0}^{\infty} a_{2t+1}\, a_{-(2t+1)} = \frac{\sigma^2}{\pi^2} \sum_{t=0}^{\infty} \int_0^{b_0^2} \frac{\xi^{2t}\, d\xi}{b_0^{2t+1}} \int_0^{b_0^2} \frac{y^{2t}\, dy}{b_0^{2t+1}}. \quad \text{(B17)}$$

The interchange of summation and integral signs is permissible since power series are uniformly convergent in any closed region within the circle of convergence. Thus

$$d_o = \frac{\sigma^2}{\pi^2 b_o^2} \int_0^{b_o^2} \int_0^{b_o^2} \sum_{t=0}^{\infty} \left(\frac{\xi^2 y^2}{b_o^4} \right)^t d\xi \, dy . \tag{B18}$$

Summing the series and performing one integration give

$$d_o = \frac{\sigma^2}{\pi^2} \int_0^{b_o^2} \tanh^{-1} \xi \, \frac{d\xi}{\xi} . \tag{B19}$$

By a similar process one can show that

$$\sum_{n=1}^{\infty} \frac{d_{2n}}{z^{2n}} = \frac{\sigma^2}{\pi^2} \int_0^{b_o^2} \frac{\xi \tanh^{-1} \xi \, d\xi}{b_o^2 z^2 - \xi^2} . \tag{B20}$$

Substitution of Equations (B19) and (B20) into Equation (B16) gives the final result:

$$\begin{aligned} F_1^{(0)}(z) = \frac{i}{8} - i \left[F_o(z) \right]^2 - i \frac{\sigma^2}{\pi^2} \int_0^{b_o^2} \tanh^{-1} \xi \, \frac{d\xi}{\xi} \\ - i \frac{2\sigma^2}{\pi^2} \int_0^{b_o^2} \frac{\xi \tanh^{-1} \xi \, d\xi}{b_o^2 z^2 - \xi^2} - 2 u_{ot} V_{ot} \\ - 2 \frac{\sigma^2}{\pi^2} \operatorname{Im} \int_0^{b_o^2} \frac{\xi \tanh^{-1} \xi \, d\xi}{b_o^2 e^{i2\psi_o} - \xi^2} . \end{aligned} \tag{B21}$$

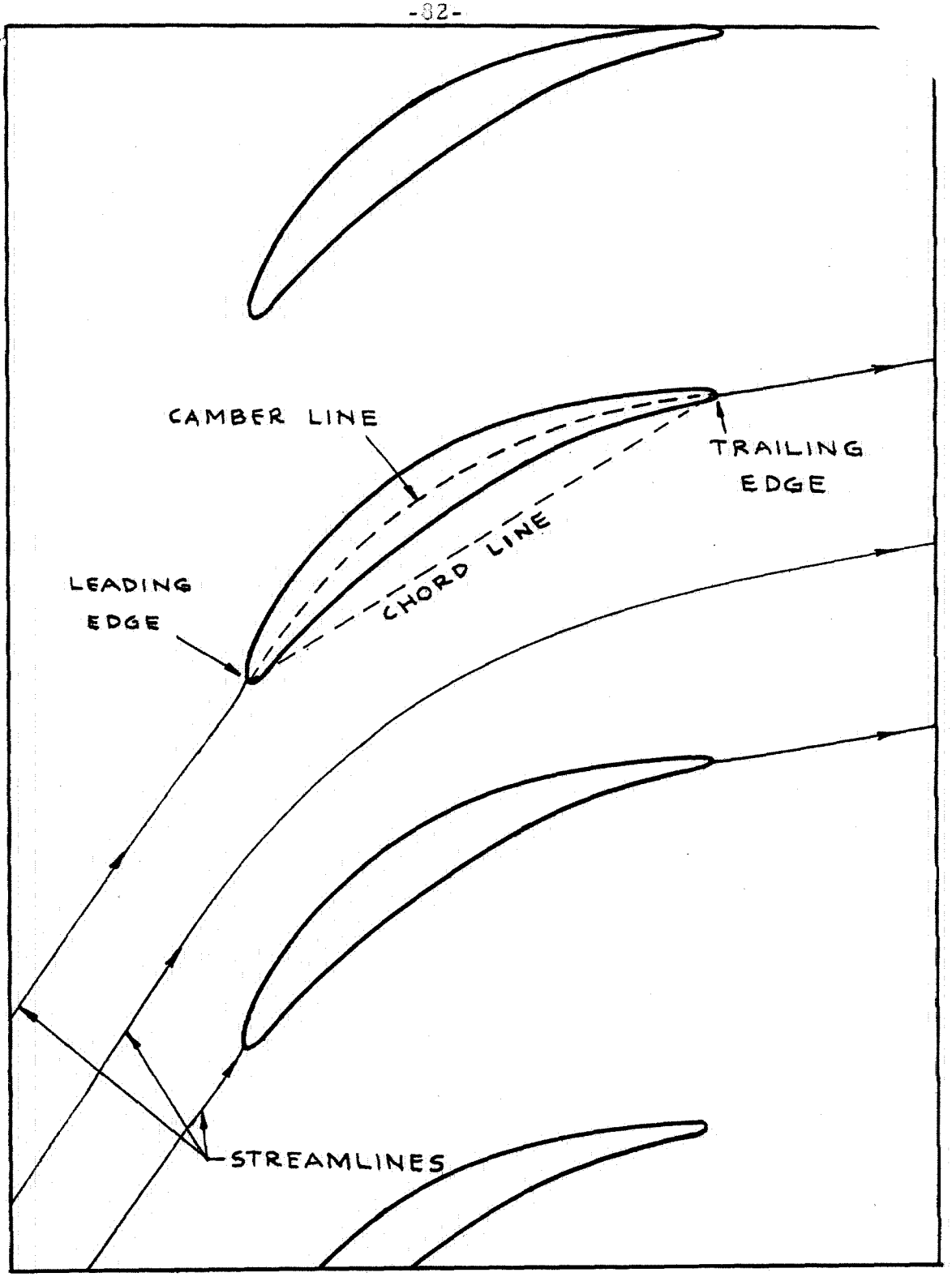

FIGURE 1

A TYPICAL COMPRESSOR CASCADE

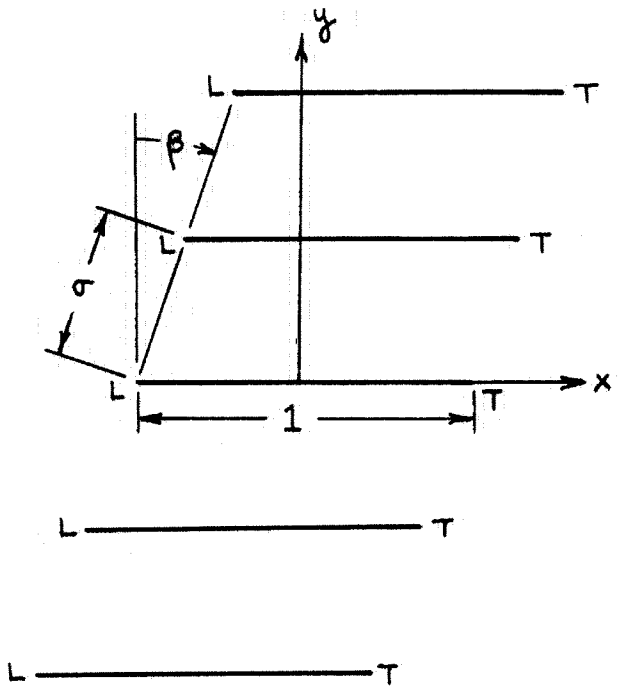

2a

PHYSICAL PLANE w

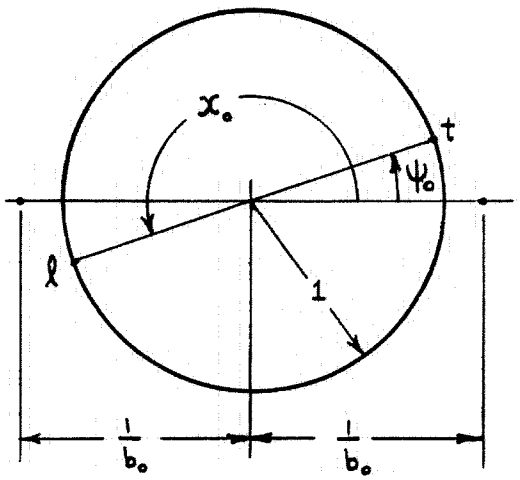

2b

CIRCLE PLANE z

FIGURE 2

FLAT PLATE CASCADE TRANSFORMATION

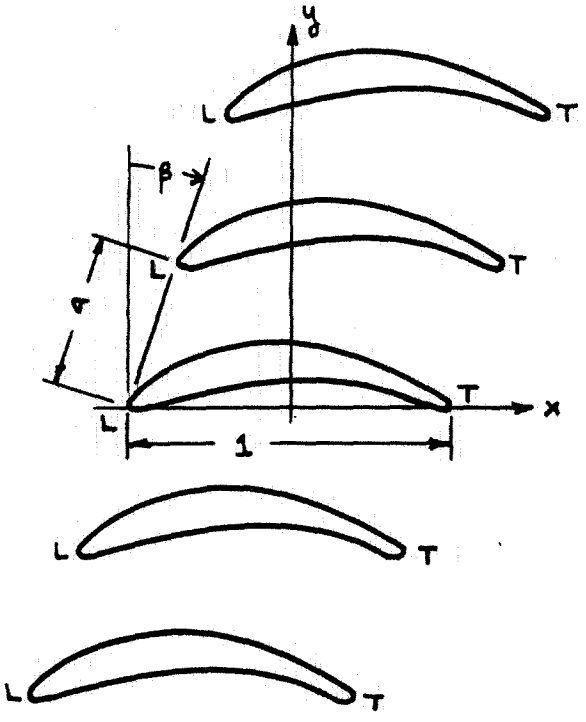

3 a

PHYSICAL PLANE W

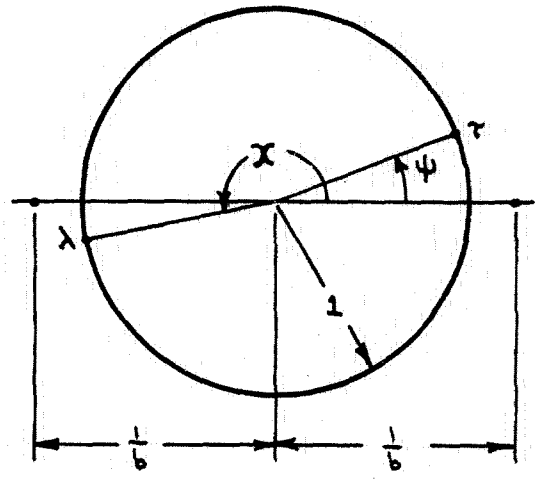

3 b

CIRCLE PLANE Z

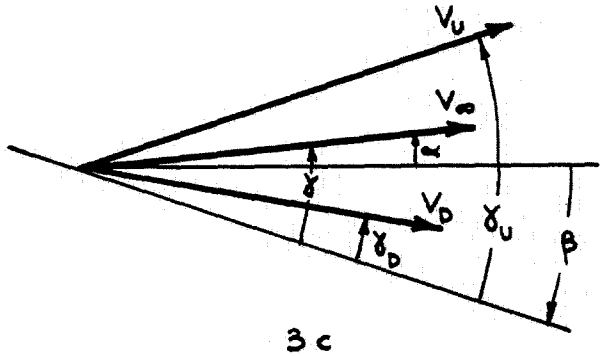

3 c

VELOCITY DIAGRAM

(PHYSICAL PLANE)

FIGURE 3

ARBITRARY CASCADE TRANSFORMATION

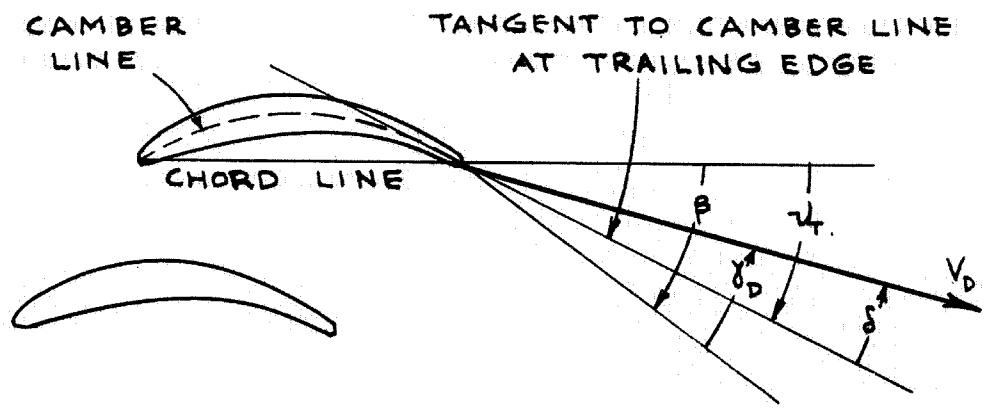

FIGURE 4

DEVIATION ANGLE δ

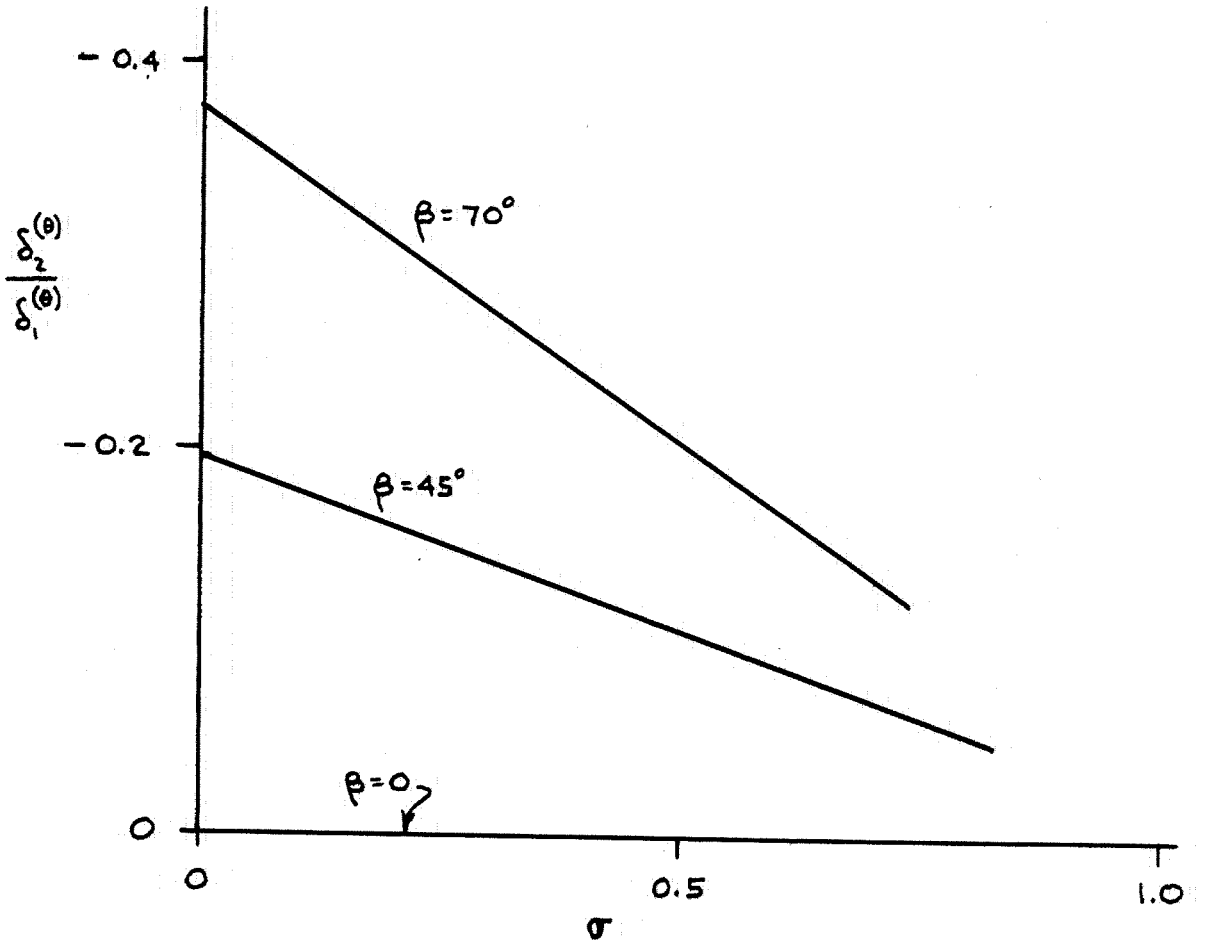

FIGURE 5

SECOND ORDER COEFFICIENT IN THE FORMULA FOR DEVIATION ANGLE

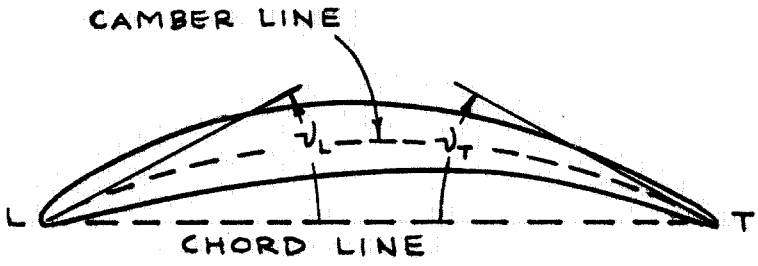

$$\theta = \nu_T + \nu_L$$

$$\mu = \nu_T - \nu_L$$

FIGURE 6

DEFINITIONS: CAMBER ANGLE θ

AND S-SHAPE ANGLE μ

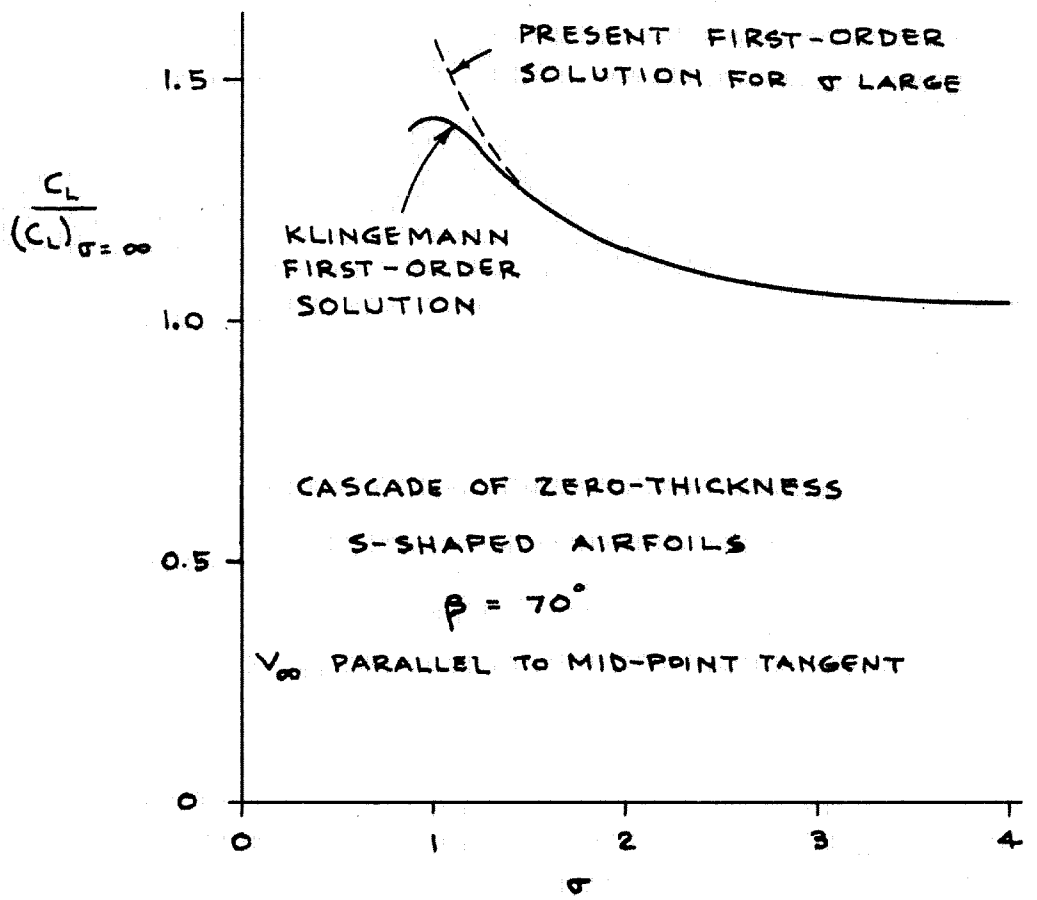

FIGURE 7

COMPARISON WITH RESULTS OF KLINGEMANN

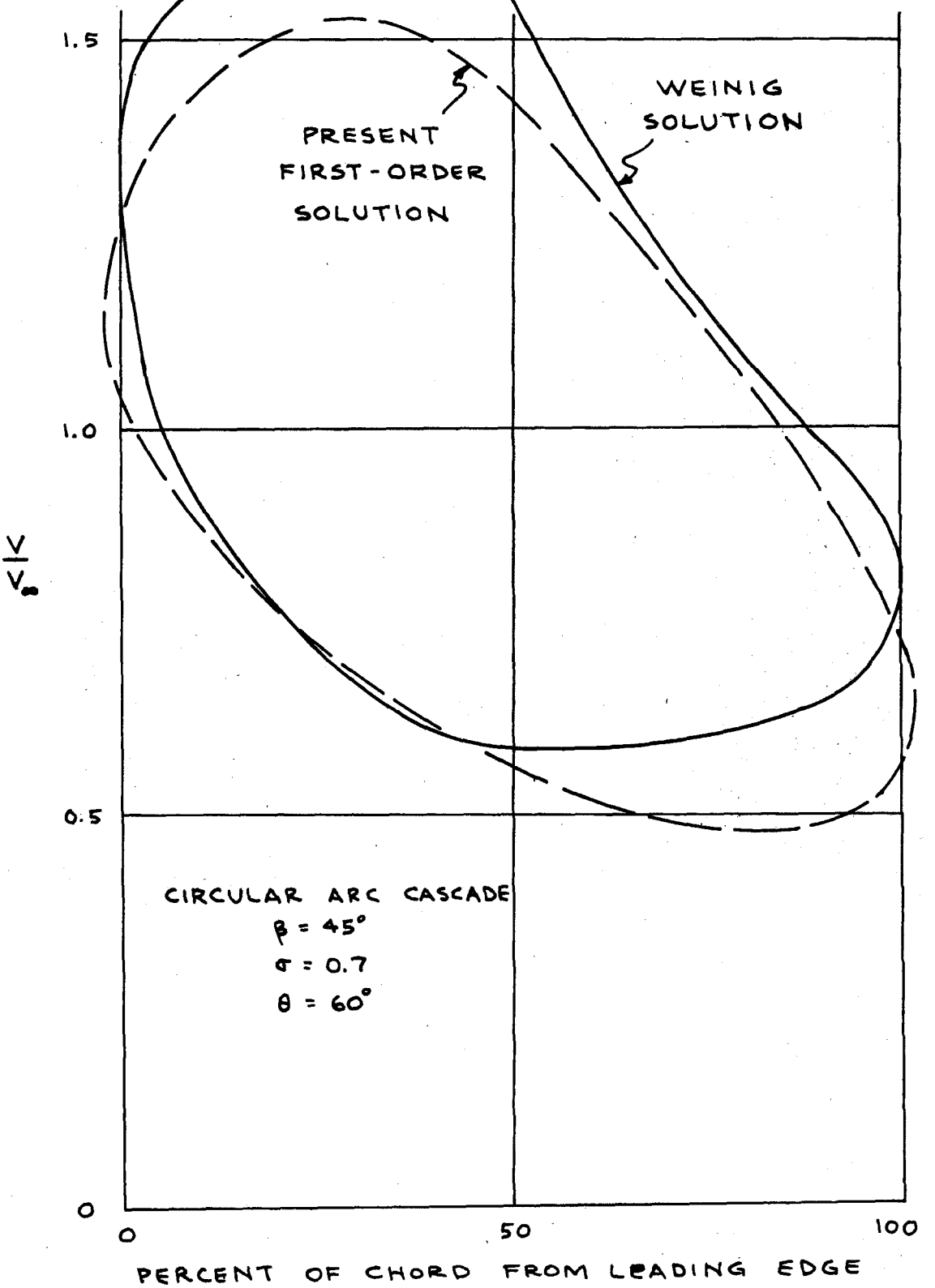

FIGURE 8 - COMPARISON WITH RESULTS OF WEINIG

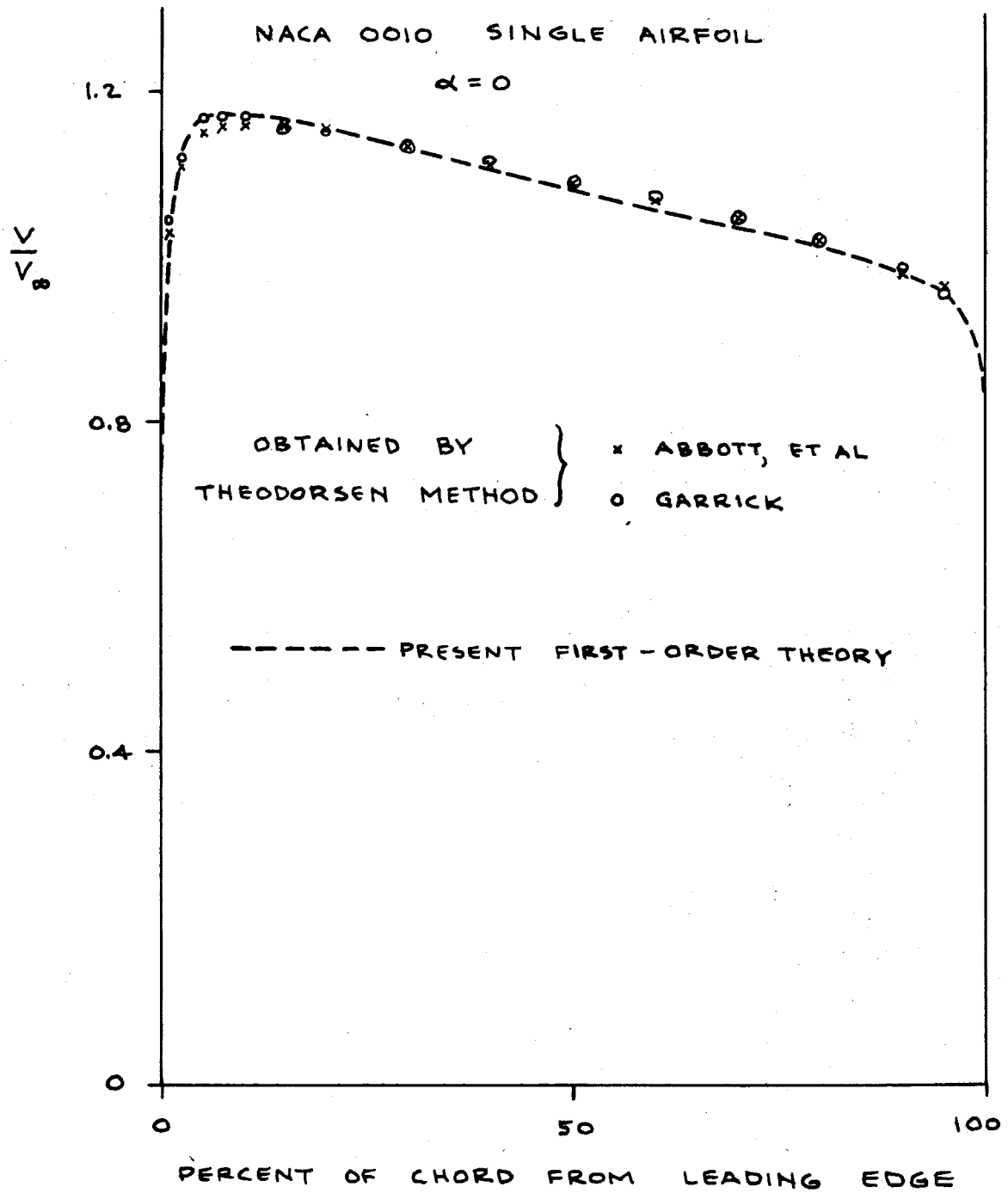

FIGURE 9

COMPARISON WITH THE THEODORSEN METHOD FOR SINGLE AIRFOILS

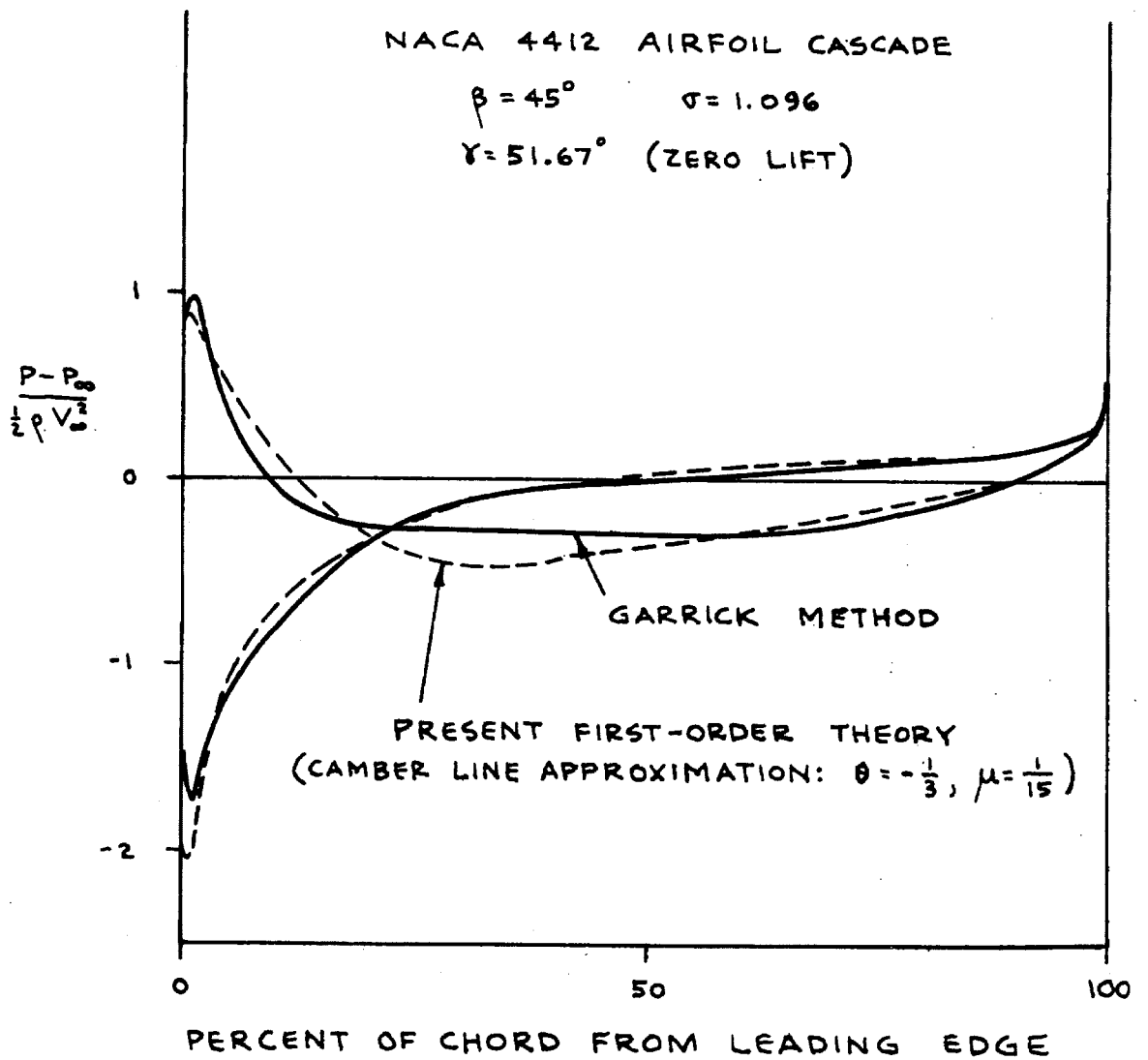

FIGURE 10

COMPARISON WITH THE GARRICK METHOD FOR CASCADES

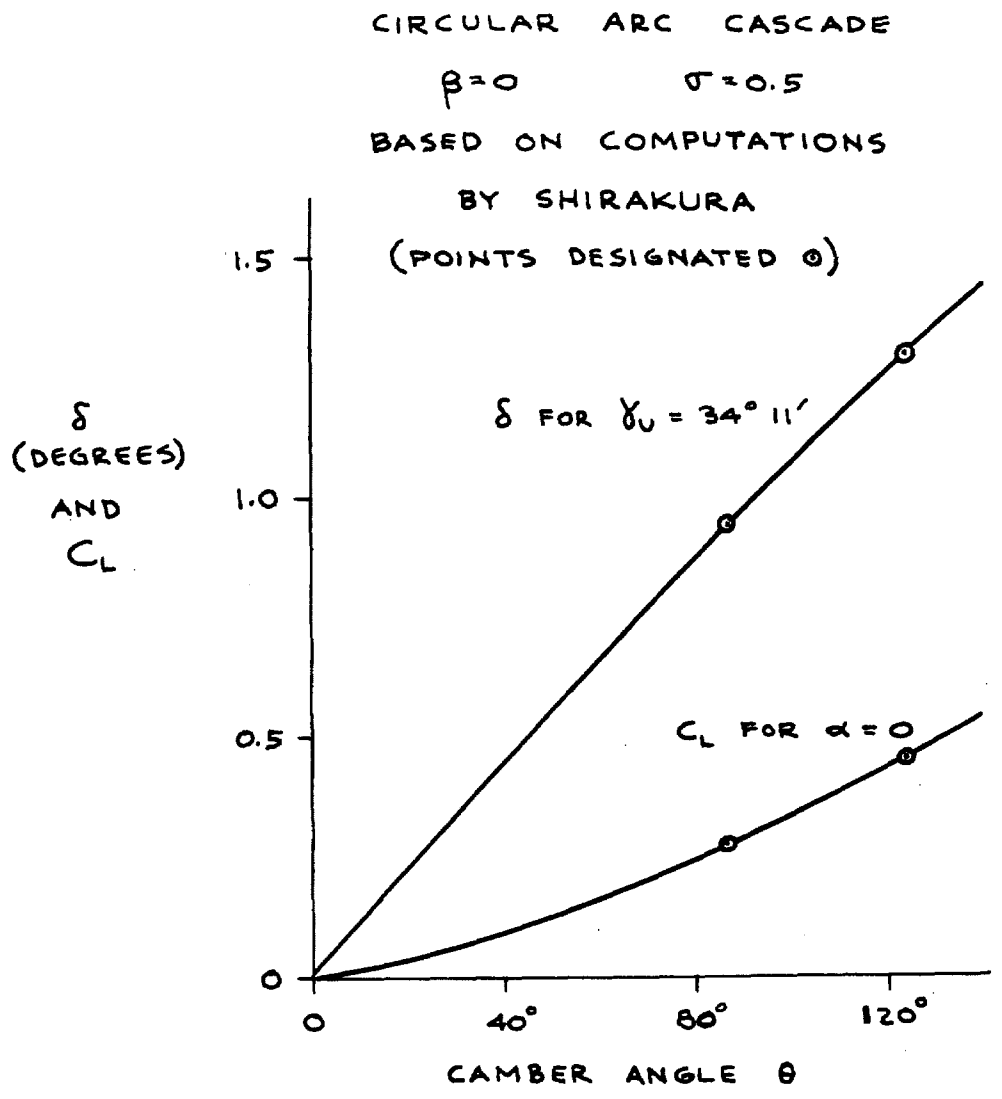

FIGURE 11

VARIATION OF DEVIATION ANGLE AND LIFT COEFFICIENT WITH CAMBER ANGLE